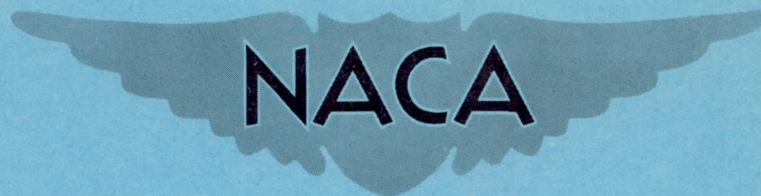


NACA RM A50101



# RESEARCH MEMORANDUM

SUMMARY REPORT OF RESULTS OBTAINED DURING DEMONSTRATION  
TESTS OF THE NORTHROP X-4 AIRPLANES

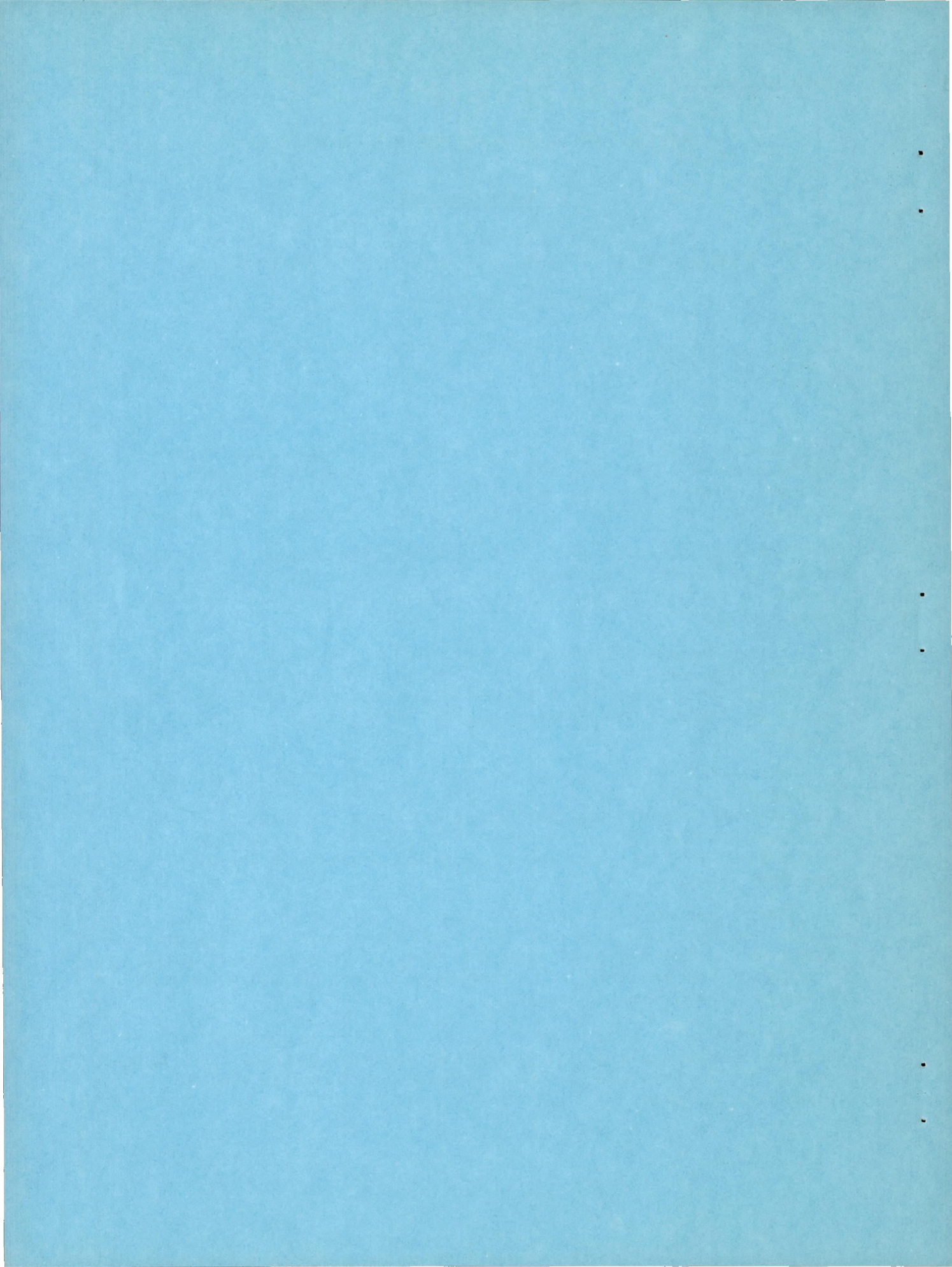
By Melvin Sadoff and Thomas R. Sisk

Ames Aeronautical Laboratory  
Moffett Field, Calif.

NATIONAL ADVISORY COMMITTEE  
FOR AERONAUTICS

WASHINGTON

December 13, 1950



## NATIONAL ADVISORY COMMITTEE FOR AERONAUTICS

RESEARCH MEMORANDUM

## SUMMARY REPORT OF RESULTS OBTAINED DURING DEMONSTRATION

## TESTS OF THE NORTHROP X-4 AIRPLANES

By Melvin Sadoff and Thomas R. Sisk

## SUMMARY

Results obtained during the demonstration flight tests of the Northrop X-4 No. 1 and No. 2 airplanes are presented. Information is included on the static and dynamic longitudinal- and lateral-stability characteristics, the stalling characteristics, and the buffet boundary.

The data indicated that the airplane was almost neutrally stable in straight flight at low Mach numbers with the center of gravity located at about 21.4 percent of the mean aerodynamic chord for the clean configuration.

In accelerated flight over a Mach number range of about 0.44 to 0.84 the airplane was longitudinally stable up to a normal-force coefficient of about 0.4. At higher values of normal-force coefficient and at the higher ( $M \approx 0.8$ ) Mach numbers a longitudinal instability was experienced.

The X-4 airplane does not satisfy the Air Force specifications for damping of the short-period longitudinal oscillation. The pilot, however, did not consider the low damping characteristics of the airplane objectionable for small disturbances. An objectionable undamped oscillation about all three axes was experienced, however, at the highest test Mach number of 0.88.

Theory predicted the period of the short-period longitudinal oscillation fairly well, while, in general, the theoretical damping indicated a higher degree of stability than was actually experienced. This discrepancy was traced to a considerable error in the estimation of the rotational damping factor.

The directional stability of the X-4 airplane as measured in steady sideslips was high and essentially constant over the speed range covered, while the dihedral effect decreased considerably with an increase in airspeed.

The damping of the lateral oscillation does not meet the Air Force requirements for satisfactory handling qualities over the Mach number range covered. The data indicated decreased damping as the flight Mach number was increased above about 0.5, and at high Mach numbers ( $M > 0.8$ ) and at high altitudes the X-4, in common with other transonic research airplanes, experienced a small amplitude undamped lateral oscillation.

The dynamic lateral-stability characteristics were estimated fairly well by theory at low Mach numbers and at a pressure altitude of 10,000 feet. At 30,000 feet, however, at Mach numbers above about 0.6, the theory again indicated a higher degree of stability than was actually obtained.

For the conditions covered in these tests the stalling characteristics of the X-4 airplane, as measured in stall approaches in straight flight and in an accelerated stall to about 1.6g, were, in general, satisfactory. Both the stall approaches and the stall were characterized by a roll-off to the right.

The X-4 buffet boundary showed a sharp drop-off in the normal-force coefficient for the onset of buffeting as the flight Mach number exceeded 0.8. The boundary was almost identical to that obtained for the D-558-II research airplane at comparable Mach numbers.

## INTRODUCTION

The X-4 airplane was constructed as part of the joint NACA - Air Force - Navy research airplane program to provide research information on the stability and control characteristics of a semitailless configuration at high subsonic Mach numbers.

In the course of the demonstration flight tests of the airplane by Northrop Aircraft, Inc., at Edwards Air Force Base, Muroc, California, limited stability and control data up to a Mach number of about 0.80 were obtained and reported in references 1 through 7. The present report consolidates the previous results and presents a limited analysis of these data. Additional information is also provided on the longitudinal-stability characteristics up to a Mach number of 0.88, the characteristics in steady sideslip at a Mach number of about 0.50, and the buffet boundary at low ( $M \approx 0.30$ ) and at high ( $M \approx 0.80$  to 0.88) Mach numbers.

## SYMBOLS

$V_i$	indicated airspeed, miles per hour
$h_p$	pressure altitude, feet

$A_Z$	normal acceleration factor (the ratio of the net aerodynamic force along the airplane Z axis to the weight of the airplane)
$A_Y$	lateral acceleration factor
$A_X$	longitudinal acceleration factor
M	Mach number
R	Reynolds number
H	total head, pounds per square foot
P	static pressure, pounds per square foot
$\Delta P$	static pressure error, pounds per square foot
q	dynamic pressure, pounds per square foot
$q_c$	impact pressure (H-P), pounds per square foot
$F_e$	stick force, pounds
$F_r$	rudder pedal force, pounds
S	wing area, square feet
M.A.C.	wing mean aerodynamic chord, feet
W	airplane weight, pounds
$H_r$	rudder hinge moment, inch-pounds
q	pitching angular velocity, radians per second
r	yawing angular velocity, radians per second
p	rolling angular velocity, radians per second
P	period of oscillation, seconds
$T_{1/2}$	time to damp to one-half amplitude, seconds
$\delta_e$	effective longitudinal control angle $\left(\frac{\delta_{eL} + \delta_{eR}}{2}\right)$ , degrees
$\delta_a$	effective lateral control angle $\left(\delta_{eL} - \delta_{eR}\right)$ , degrees

$\delta_r$	rudder angle, degrees
$\beta$	sideslip angle, degrees
$C_N$	normal-force coefficient $\left(\frac{WA_Z}{qS}\right)$
$F_e/q$	stick-force factor, feet squared
$C_{m\alpha}$	static stability parameter
$C_{m\dot{q}} + C_{m\ddot{\alpha}}$	rotational damping parameter

#### Subscripts

L	left elevon
R	right elevon
T	true
r	recorded

#### AIRPLANE

The Northrop X-4 airplane is a semitailless research airplane having a vertical-tail but no horizontal-tail surface. It is powered by two Westinghouse J-30-WE-7-9 engines and is designed for flight research in high subsonic speed range. A three-view drawing of the airplane is presented as figure 1 and photographs of the airplane are shown in figure 2. The physical characteristics of the airplane are listed in table I.

#### INSTRUMENTATION

Standard NACA instruments were used to record the altitude, airspeed, right- and left-elevon positions, rudder position, and sideslip angle on the X-4 No. 1 airplane; and these same quantities plus the normal, longitudinal, and lateral accelerations, the pitching and rolling angular velocities, the stick force, pedal force, and the elevon and rudder hinge moments were used on the X-4 No. 2 airplane. In addition, the normal acceleration, altitude, airspeed, right- and left-elevon positions, and rudder position on the No. 2 airplane were telemetered to a ground station.

All the internal records were correlated by a common timer. Since it was not possible to calibrate and maintain the hinge-moment instrumentation properly, the data were unreliable and are not presented.

The airspeed and altitude recorder was connected to the airspeed head on the vertical fin. This installation was calibrated by the "fly-by" method on the X-4 No. 1 airplane up to a Mach number of about 0.50. Subsequently, an airspeed calibration was made on the X-4 No. 2 airplane over a Mach number range of 0.70 to 0.88 using the radar method described in reference 8. The results of these calibrations are presented in figures 3 and 4 which show, respectively, the static pressure error ratio  $\Delta P/q_c$  at low lift coefficients ( $A_Z = 1.0$ ) as a function of true Mach number and the variation of true Mach number  $M_T$  with recorded Mach number  $M_r$ . Included for comparison with the X-4 data in figure 3 are the results from reference 9 of a calibration of a static tube ahead of the vertical tail of a free-fall model of a canard airplane at low lift coefficients.

## TESTS, RESULTS, AND DISCUSSION

### Longitudinal-Stability Characteristics

Straight flight.— The static longitudinal-stability characteristics in straight flight were measured in the clean configuration at indicated airspeeds varying from 140 to about 400 miles per hour and at pressure altitudes between 10,000 and 20,000 feet. The center of gravity for these tests ranged from 18.0 to about 21.6 percent of the mean aerodynamic chord. Data were also obtained from the gear-down flaps-up configuration at indicated airspeeds between 145 and 215 miles per hour and at pressure altitudes between 2,200 and 15,000 feet with the center of gravity varying from 19.5 to 22.0 percent of the mean aerodynamic chord.

The results of these tests are presented in figure 5 for the several center-of-gravity positions. It may be noted that only approximate center-of-gravity positions are given since, because of the uncertainty of the exact sequence of fuel emptying from the wing tanks, they are not known to within an estimated  $\pm 0.5$  percent mean aerodynamic chord. The results presented in figure 5 for the several center-of-gravity positions are consistent within the accuracy of the data. The data indicate that the airplane was almost neutrally stable at the higher indicated speeds or low normal-force coefficients with the center of gravity at about 21.4 percent of the mean aerodynamic chord. It was indicated that the stability tended to increase as the normal-force coefficient was increased. It was also indicated that lowering the landing gear had little effect on the longitudinal stability.

Accelerated flight.— The longitudinal-stability characteristics in accelerated flight were measured in steady or wind-up turns and in gradual pull-ups. The data were obtained at a Mach number of 0.44 at 10,000 feet, at several Mach numbers from 0.5 to about 0.8 at 20,000 feet, and at several Mach numbers from 0.70 to 0.86 at 30,000 feet.<sup>1</sup> In general, at 10,000 and 20,000 feet the data presented for values of normal acceleration less than 2g were obtained in steady turns, while the data for values of normal acceleration greater than 2g were obtained in steady or wind-up turns. The center of gravity for these tests was located at about 18.5 percent of the mean aerodynamic chord.

Time histories of two typical test runs are presented in figure 6. It is interesting to note in this figure that, while the stick-force data show decreasing values, the elevon angle and normal-force coefficient continue to increase. The apparent stick-free instability within each run was probably due to the friction and inertia forces in the hydraulic-boost elevon system wherein the elevons continued to move in the direction of stick movement after the stick motion had stopped. Because of this characteristic, the stick-free data may be expected to exhibit more scatter than the stick-fixed data. The stick-free data are shown in figure 7 as a matter of interest although they are not analyzed further because of the uncertainty regarding the characteristics of the mechanical feel and the hydraulic boost utilized in the elevon control system. Figure 7 shows the variation of elevon control angle with normal-force coefficient and the variation of elevon stick force with normal acceleration for the several Mach numbers and altitudes. These data indicate that for values of normal-force coefficient up to about 0.4 over a Mach number range of 0.44 to 0.84 the airplane is longitudinally stable stick fixed and stick free. Above a Mach number of about 0.8, however, the airplane becomes longitudinally unstable at values of normal-force coefficient above about 0.4. (It should be noted, however, that the higher range of normal-force coefficient was not explored between Mach numbers of 0.5 and 0.8.) The instability is clearly shown by the data in figure 8 which present the variation of elevon control angle with normal-force coefficient for the several runs where longitudinal instability was encountered. It should be noted that the data above a normal-force coefficient of 0.4 are not strictly valid points since the airplane was pitching up rapidly at the time. It may be observed in this figure that the instability occurred at a normal-force coefficient of about 0.42 at Mach numbers of about 0.82 and at a normal-force coefficient of about 0.38 at a Mach number of 0.84. A typical time history of a run in which longitudinal instability was experienced is presented in figure 9.

---

<sup>1</sup> The data at  $M = 0.70$  were obtained in straight flight during the radar airspeed calibration runs. The data were extrapolated to a  $C_N$  of 0.4 by using the elevon-angle gradient determined at 20,000 feet pressure altitude.

---



From the results presented in figure 7, the elevon angles required for balance for several values of  $C_N$  were derived as a function of Mach number and are shown in figure 10 for altitudes of 10,000 and 20,000 feet, and for 30,000 feet. Also presented for comparison with the experimental values are the angles estimated from the wind-tunnel data of reference 10. The experimental results at 10,000 and 20,000 feet show little change in the elevon angles for balance over the entire range of Mach number from 0.44 to about 0.82. At 30,000 feet, the experimental data show a slight diving tendency as the flight Mach number is increased above 0.82. The estimated elevon angles compare favorably with the experimental values at 10,000 and 20,000 feet. At 30,000 feet, the agreement is not quite as good, although the trends agree fairly well, especially at the higher values of normal-force coefficient. The estimated data, however, tend to exaggerate the diving tendency.

A measure of the stick-fixed stability  $d\delta_e/dC_N$  is plotted as a function of Mach number in figure 11. The estimated values from the data of reference 10 are also included. Both the experimental and the estimated data indicate an increase in stability of approximately the same magnitude as the Mach number exceeds 0.8.

Dynamic stability.— The dynamic longitudinal-stability characteristics of the X-4 airplane were obtained in longitudinal oscillations which were excited by abruptly deflecting the elevon control and returning it to the trim position. These oscillations were obtained at Mach numbers of about 0.50 and 0.80 at 20,000 feet and at Mach numbers between 0.82 and 0.86 at 30,000 feet. Time histories of two representative oscillations are given in figure 12. Although these data show that for Mach numbers from 0.50 to 0.86 the X-4 airplane does not meet the requirements for satisfactory damping of the longitudinal short-period oscillation which stipulates that the oscillation damp to one-tenth amplitude in one cycle (reference 11), the pilot did not consider the low damping of the airplane objectionable for small disturbances. At the highest test Mach number reached during the demonstration tests ( $M=0.88$ ), an objectionable undamped oscillation about all three axes was experienced which indicated that the dynamic longitudinal and lateral stability were about neutral at this Mach number at 30,000 feet pressure altitude. A time history of several of the pertinent measured quantities for this run is given in figure 13. The period  $P$  and the time to damp to one-half amplitude  $T_{1/2}$  were determined from these oscillations and others not presented here, and are presented as a function of Mach number in figure 14. The theoretical period and damping computed by the methods of reference 12 are also presented in this figure. It may be seen from figure 14 that the period is estimated fairly well by the theory. The theoretical damping, however, increases considerably as the flight Mach number is increased, while the experimental results show only a small increase in damping at 20,000 feet and actually a rapid decrease in damping above a Mach number of 0.86 at 30,000 feet.

In an attempt to determine the reasons for the fairly good agreement in period and the relatively poor agreement for the damping, values of the static stability parameter  $C_{m\alpha}$  and the rotational damping coefficient  $C_{mq} + C_{m\dot{\alpha}}$  were derived from the experimental oscillations by the use of the equations given in reference 13. The results of these computations are presented in figure 15 as functions of Mach number. Also included in this figure for comparison with the derived data are the wind-tunnel values of  $C_{m\alpha}$  (reference 10) and the values of  $C_{mq}$  estimated by the methods of reference 14. Two important observations may be made from figure 15. First, as compared to the wind-tunnel data, the flight results indicate a lower degree of static stability over most of the Mach number range and, within the experimental scatter of the flight data, the stability appears to be essentially constant over the Mach number range. Second, the values of rotational damping factor  $C_{mq} + C_{m\dot{\alpha}}$  derived from the flight results are considerably lower than the estimated values of  ${}^2C_{mq}$  and, while the estimated values of  $C_{mq}$  remain approximately constant at a value of  $-1.5$ , the experimental values decrease from a value of  $-0.5$  at a Mach number of  $0.5$  to zero at Mach numbers around  $0.8$ . At the highest test Mach number of  $0.88$  the damping factor  $C_{mq} + C_{m\dot{\alpha}}$  corresponding to the undamped oscillation described previously assumes a relatively large positive value (negative damping in pitch) and of the same magnitude as that contributed by the airplane lift-curve slope.

To illustrate the importance of properly accounting for the damping-in-pitch factor in the theoretical computations, the values of  $C_{mq} + C_{m\dot{\alpha}}$  derived from the flight data were used to recompute the variation with Mach number of the time required for the longitudinal short-period oscillation to damp to one-half amplitude. The results which are presented in figure 16 show, as expected, that the experimental and theoretical values of  $T_{1/2}$  are brought into very good agreement. It should be noted in this figure that the time to damp to one-half amplitude still has a moderate finite value even though the rotational damping factor  $C_{mq} + C_{m\dot{\alpha}}$  approaches zero at Mach numbers around  $0.80$ .

#### Lateral- and Directional-Stability Characteristics

In steady sideslips.— The lateral- and directional-stability characteristics in steady sideslips were measured at indicated airspeeds of about 175 to 280 miles per hour at approximately 15,000 feet and at an indicated airspeed of about 260 miles per hour at 20,000 feet. The results of these measurements are shown in figure 17 which gives the variation of the effective longitudinal control angle, the effective

---

<sup>2</sup> It is assumed that for tailless airplanes  $C_{m\dot{\alpha}}$  is negligible.

---

lateral control angle, and the rudder angle as a function of sideslip angle. Several interesting observations may be made from this figure, notably that an increase in nose-down trim occurs as the sideslip angle is increased; the directional stability is high and remains essentially constant over the airspeed range covered; and the effective dihedral decreases considerably with increase in airspeed from 175 to 280 miles per hour. The measure of directional stability  $d\delta_r/d\beta$  has an average value of about 1.80 as compared with a value of 2.0 obtained from the wind-tunnel data of reference 15. The effective dihedral, as measured by the rate of change of lateral control angle with sideslip angle  $d\delta_a/d\beta$ , varies from a value of 0.28 at 280 miles per hour to 0.69 at 175 miles per hour. The variation of the effective dihedral with normal-force coefficient is given in figure 18. The values estimated from the wind-tunnel data in reference 15 are also presented in this figure. The agreement between the flight and wind-tunnel measurements is considered good. No corrections were applied to the wind-tunnel data for the effect of rudder deflection.

Dynamic stability.— The dynamic lateral-stability characteristics were obtained from oscillations which were initiated by abruptly deflecting the rudder and returning it to the trim position and by deflecting and then releasing the rudder. These oscillations were obtained in the clean configuration at 10,000 feet for a range of normal-force coefficients of 0.2 to about 0.55 corresponding to a Mach number range of 0.25 to 0.4 and at 30,000 feet over a Mach number range of 0.5 to 0.73. Oscillations were also obtained for the gear-down configuration at 10,000 feet at normal-force coefficients between 0.3 and 0.45 corresponding to Mach numbers of about 0.3. Typical time histories of the lateral oscillations obtained are shown in figure 19. From these oscillations and others not presented herein the period and time to damp to one-half amplitude were determined and are presented in figure 20. These results show that the X-4 airplane does not meet the Air Force damping requirements for satisfactory handling qualities, although for the gear-down configuration at 10,000 feet the characteristics are close to the satisfactory region. The period and time to damp to one-half amplitude are replotted as a function of normal-force coefficient in figure 21(a) and as a function of Mach number in figure 21(b). Also presented in this figure are the theoretical values of period and damping computed by the methods of reference 16. A comparison of the experimental with the theoretical results indicates, in general, good agreement of the periods and fair agreement of the damping at low altitudes and low Mach numbers. At 30,000 feet, however, the theory indicates a decreasing time required to damp to one-half amplitude as the Mach number is increased above 0.5, while the experimental results indicate a rapid deterioration of the damping. As noted previously in connection with figure 13, the damping tends to zero as the flight Mach number approaches 0.88. It may be of interest to mention that the test point at 30,000 feet and at about 0.73 Mach number was obtained from an unusual oscillation which abruptly changed its period and damping

characteristics. (See fig. 22.) Although the period and damping variations shown in this figure may be explained by fuel sloshing and gyroscopic coupling of the lateral motions with the short-period longitudinal oscillation (reference 17), further testing is considered necessary before any definite conclusions can be made regarding the exact nature of these oscillations.

### Stalling Characteristics

The stalling characteristics of the X-4 were determined from stall approaches made in the clean and in the gear-down configuration in lg flight with the engine rpm set for 11,000 and from an accelerated stall made in the clean configuration with the engine rpm set for 13,000. (Rated rpm is 17,200.) The pressure altitude for these stalls was about 17,000 feet and the corresponding Reynolds number approximately  $9 \times 10^6$ . As a safety measure, an AAF spin chute was installed during these tests.

The results showed that the unaccelerated stall approaches were characterized by a mild dropping of the right wing. Recovery was readily effected by a small forward movement of the stick. The accelerated stall was characterized by a fairly violent roll-off to the right and by moderate buffeting which occurred at the stall and persisted through most of the recovery. Recovery was again easily and rapidly accomplished by a small forward stick movement. A time history of the motions of the airplane and the controls during the accelerated stall is given in figure 23 to illustrate the above points. In this time history the stall is considered to occur at approximately 4.4 seconds, at which point a considerable increase in elevon angle resulted in no increase in  $A_z$  (or  $C_N$ ). Rapid aileron motion at this time, which failed to check the right roll, is evident.

A comparison of the peak values of normal-force coefficient obtained in flight with the values of  $C_{L_{max}}$  obtained from two-dimensional and three-dimensional wind-tunnel tests is presented in figure 24. In evaluating this comparison, differences in the flight and wind-tunnel values of Reynolds number and elevon-angle setting and the dynamic effects on maximum lift should be considered. The Reynolds number and the dynamic effect differences are such as to increase the flight values of  $C_{N_{max}}$  relative to the wind-tunnel values, and the difference in elevon angle reduces the flight  $C_{N_{max}}$  approximately 0.1 relative to the wind-tunnel values. There is also shown in figure 24 the Mach numbers and normal-force coefficients at which the longitudinal instability occurred in flight. These are included to show the possible limiting values of normal-force coefficient that may be reached with this airplane.

It is of interest to note in connection with the longitudinal-stability characteristics at high lift coefficients that no instability was encountered up to normal-force coefficients of about 0.73 and 0.84 for the stall approaches and the stall, respectively. The accelerated stability data, on the other hand, indicated that longitudinal instability was experienced at normal-force coefficients around 0.4 at high ( $M \approx 0.8$ ) Mach numbers. A possible explanation for this is that the boundary-layer fences with which the X-4 is equipped become less effective in preventing the instability as the Mach number is increased above the speeds at which the stall tests were run ( $M \approx 0.3$ ).

### Buffet Boundary

During the course of the stall tests at about 17,000 feet and accelerated stability tests at 20,000 and 30,000 feet, some limited information on the buffet boundary of the X-4 airplane was obtained. The data which were only available at low ( $M \approx 0.3$ ) and at high ( $M \approx 0.8$  to 0.88) Mach numbers are shown in figure 25. The complete buffet boundary for the D-558-II airplane (reference 19) is also included in this figure for comparison with the X-4 results. The data for both airplanes indicate a fairly rapid drop in the normal-force coefficient  $C_N$  at which buffeting first occurs as the flight Mach number exceeds about 0.8, although the X-4 boundary is slightly lower than the D-558-II at comparable Mach numbers. An indication of the extent of penetration into the buffet region is shown by the peak  $C_N$  values reached during the X-4 demonstration tests (circled points, fig. 25). Another point of interest in figure 25 is that the normal-force coefficients and Mach numbers at which the longitudinal instability was observed very nearly coincide with the buffet boundary. The reason for this coincidence is not entirely obvious, although it may be reasonable to expect that the breakdown of flow over the wing which results in buffeting also produces the adverse aerodynamic-loading changes which cause the instability.

### CONCLUSIONS

From the results obtained during the demonstration flight tests of the Northrop X-4 No. 1 and No. 2 airplanes and from a comparison of these results with estimated and theoretical data, the following conclusions were drawn:

1. The airplane was almost neutrally stable in straight flight at low Mach numbers with the center of gravity located at about 21.4 percent of the mean aerodynamic chord for the clean configuration. Lowering the landing gear had no significant effect on the longitudinal stability.

There was some indication that the stability tended to increase for both configurations as the normal-force coefficient was increased.

2. The airplane was longitudinally stable in accelerated flight over a Mach number range of 0.44 to about 0.84 up to a normal-force coefficient of about 0.4. At higher values of normal-force coefficient and at Mach numbers of about 0.8 a longitudinal instability was experienced.

3. The airplane does not meet the Air Force specifications for the damping of the short-period longitudinal oscillations. The pilot, however, did not object to the low damping for small amplitude oscillations. However, an objectionable undamped oscillation about all three axes was experienced at the highest test Mach number of about 0.88 which may well limit the X-4 airplane to this speed.

4. The theory predicted the period of the short-period longitudinal oscillation fairly well, while, in general, the theoretical damping indicated a higher degree of stability than was actually experienced. This disagreement was traced to a large error in the estimation of the rotational damping factor.

5. The directional stability of the airplane was high and essentially constant over the speed range considered, while the effective dihedral increased considerably with an increase in normal-force coefficient. The lateral- and directional-stability characteristics estimated from wind-tunnel data compared favorably with the flight results.

6. The damping of the lateral oscillation does not meet the Air Force requirements for satisfactory handling qualities.

7. The dynamic lateral-stability characteristics were estimated fairly well by the theory at low Mach numbers at a pressure altitude of 10,000 feet. At 30,000 feet, however, and at Mach number above about 0.6, the theory indicated a higher degree of stability than was actually experienced.

8. For the conditions covered in these tests, the stalling characteristics of the airplane at low Mach numbers were, in general, satisfactory. The stall was characterized by a roll-off to the right and by moderate buffeting which served as a stall warning.

9. The buffet boundary for the X-4 airplane, which was almost identical to that for the D-558-II airplane, showed a sharp drop-off in the normal-force coefficient for the onset of buffeting as the Mach number exceeded about 0.8.

Ames Aeronautical Laboratory,  
National Advisory Committee for Aeronautics,  
Moffett Field, Calif.

## REFERENCES

1. Drake, Hubert M.: Stability and Control Data Obtained from First Flight of X-4 Airplane. NACA RM L9A31, 1949.
2. Williams, Walter C.: Results Obtained from Second Flight of X-4 Airplane (A.F. No. 46-676). NACA RM L9F21, 1949.
3. Williams, Walter C.: Results Obtained from Third Flight of Northrop X-4 Airplane (A.F. No. 46-676). NACA RM L9G20a, 1949.
4. Valentine, George M.: Stability and Control Data Obtained from Fourth and Fifth Flights of the X-4 Airplane (A.F. No. 46-676). NACA RM L9G25a, 1949.
5. Matthews, James F., Jr.: Results Obtained During Flights 1 to 6 of the Northrop X-4 Airplane (A.F. No. 46-676). NACA RM L9K22, 1950.
6. Sadoff, Melvin, and Sisk, Thomas R.: Stall Characteristics Obtained from Flight 10 of Northrop X-4 No. 2 Airplane (A.F. No. 46-677). NACA RM A50A04, 1950.
7. Sadoff, Melvin, and Sisk, Thomas R.: Longitudinal-Stability Characteristics of the Northrop X-4 Airplane (A.F. No. 46-677). NACA RM A50D27, 1950.
8. Zalovecik, John A.: A Radar Method of Calibrating Airspeed Installations on Airplanes in Maneuvers at High Altitudes and at Transonic and Supersonic Speeds. NACA TN 1979, 1949.
9. Kraft, Christopher C., Jr., and Mathews, Charles W.: Determination by the Free-Fall Method of the Longitudinal Stability and Control Characteristics of a Canard Model at Transonic Speeds. NACA RM L50D04, 1950.
10. Preliminary Report on High-Speed Wind-Tunnel Tests of a 1/4th-Scale Reflection Plane Model of the Northrop XS-4 Airplane. Southern California Cooperative Wind-Tunnel Report No. 69, Oct. 28, 1948.
11. Anon.: Flying Qualities of Piloted Airplanes. AAF Specification No. 1815-B, 1 June, 1948.
12. Greenberg, Harry, and Sternfield, Leonard: A Theoretical Investigation of Longitudinal Stability of Airplanes with Free Controls Including Effect of Friction in Control System. NACA Rep. 791, 1944.

13. Gillis, Clarence L., Peck, Robert F., and Vitale, James A.: Preliminary Results from a Free-Flight Investigation at Transonic and Supersonic Speeds of the Longitudinal Stability and Control Characteristics of an Airplane Configuration with a Thin Straight Wing of Aspect Ratio 3. NACA RM L9K25a, 1950.
14. Toll, Thomas A., and Queijo, M. J.: Approximate Relations and Charts for Low-Speed Stability Derivatives of Swept Wings. NACA TN 1581, 1948.
15. Pass, H. R., and Hayes, B. R.: Wind-Tunnel Tests of a 1/4-Scale Model of the Northrop XS-4 Airplane. Northrop Report No. A-WT-46, Dec. 1947.
16. Sternfield, Leonard, and Gates, Ordway B., Jr.: A Method of Calculating a Stability Boundary That Defines a Region of Satisfactory Period-Damping Relationship of the Oscillatory Mode of Motion. NACA TN 1859, 1949.
17. Amster, W.: Analysis of Flight Test Lateral Dynamic Stability Data. Northrop Rep. No. AM-109, Oct. 1949.
18. Polentz, Perry P.: Comparison of the Aerodynamic Characteristics of the NACA 0010 and 0010-64 Airfoil Sections at High Subsonic Mach Numbers. NACA RM A9G19, 1949.
19. Mayer, John P., and Valentine, George M.: Flight Measurements with the D-558-II (BuAero No. 37974) Research Airplane Measurements of the Buffet Boundary and Peak Airplane Normal-Force Coefficients at Mach Numbers up to 0.90. NACA RM L50E31, 1950.



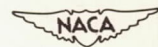
TABLE I. - PHYSICAL CHARACTERISTICS OF X-4 AIRPLANE

Engines (two) . . . . .	Westinghouse J-30-WE-7-9
Rating (each) static thrust at sea level, pounds . . . . .	1600
Airplane weight (average for flights 12, 13, and 15), pounds	
Maximum (238 gal fuel) . . . . .	7847
Minimum (10 gal trapped fuel) . . . . .	6477
Wing loading (average for flights 12, 13, and 15), pounds per square foot	
Maximum . . . . .	39.2
Minimum . . . . .	32.4
Center-of-gravity travel (average for flights 12, 13, and 15) percent M. A. C.	
Gear up, full load . . . . .	19.10
Gear up, post flight . . . . .	17.10
Gear down, full load . . . . .	19.40
Gear down, post flight . . . . .	17.50
Height, over-all feet . . . . .	14.83
Length, over-all feet . . . . .	23.25
Wing	
Area, square feet . . . . .	200
Span, feet . . . . .	26.83
Airfoil section . . . . .	NACA 0010-64
Mean aerodynamic chord, feet . . . . .	7.81
Aspect ratio . . . . .	3.6
Root chord, feet . . . . .	10.25
Tip chord, feet . . . . .	4.67
Taper ratio . . . . .	2.2:1
Sweepback (leading edge), degrees . . . . .	41.57
Dihedral (chord plane), degrees . . . . .	0
Wing boundary-layer fences	
Length, percent local chord . . . . .	30.0
Height, percent local chord . . . . .	5.0
Location, percent semispan . . . . .	90.0



TABLE I.— CONCLUDED

Wing flaps (split)	
Area, square feet . . . . .	16.7
Span, feet . . . . .	8.92
Chord, percent wing chord . . . . .	25
Travel, degrees . . . . .	30
Dive brake dimensions as flaps	
Travel, degrees . . . . .	±60
Elevons	
Area (total), square feet . . . . .	17.20
Span (2 elevons), feet . . . . .	15.45
Chord, percent wing chord . . . . .	20
Movement, degrees	
Up . . . . .	35
Down . . . . .	20
Operation	Hydraulic with electrical emergency
Vertical Tail	
Area, square feet . . . . .	16
Height, feet . . . . .	5.96
Rudder	
Area, square feet . . . . .	4.1
Span, feet . . . . .	4.3
Travel, degrees . . . . .	±30
Operation . . . . .	Direct



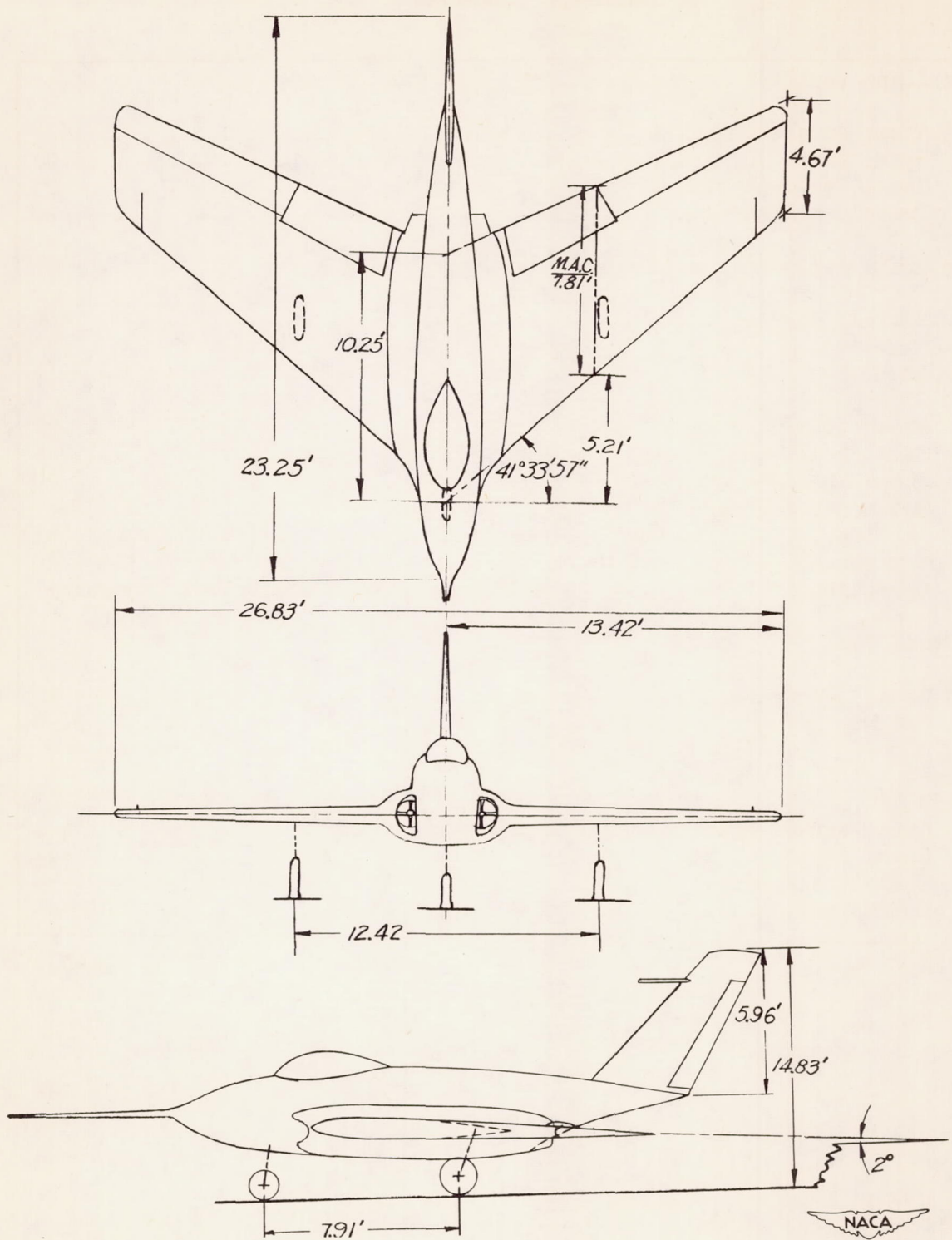


Figure 1.- Three-view drawing of X-4 airplane.

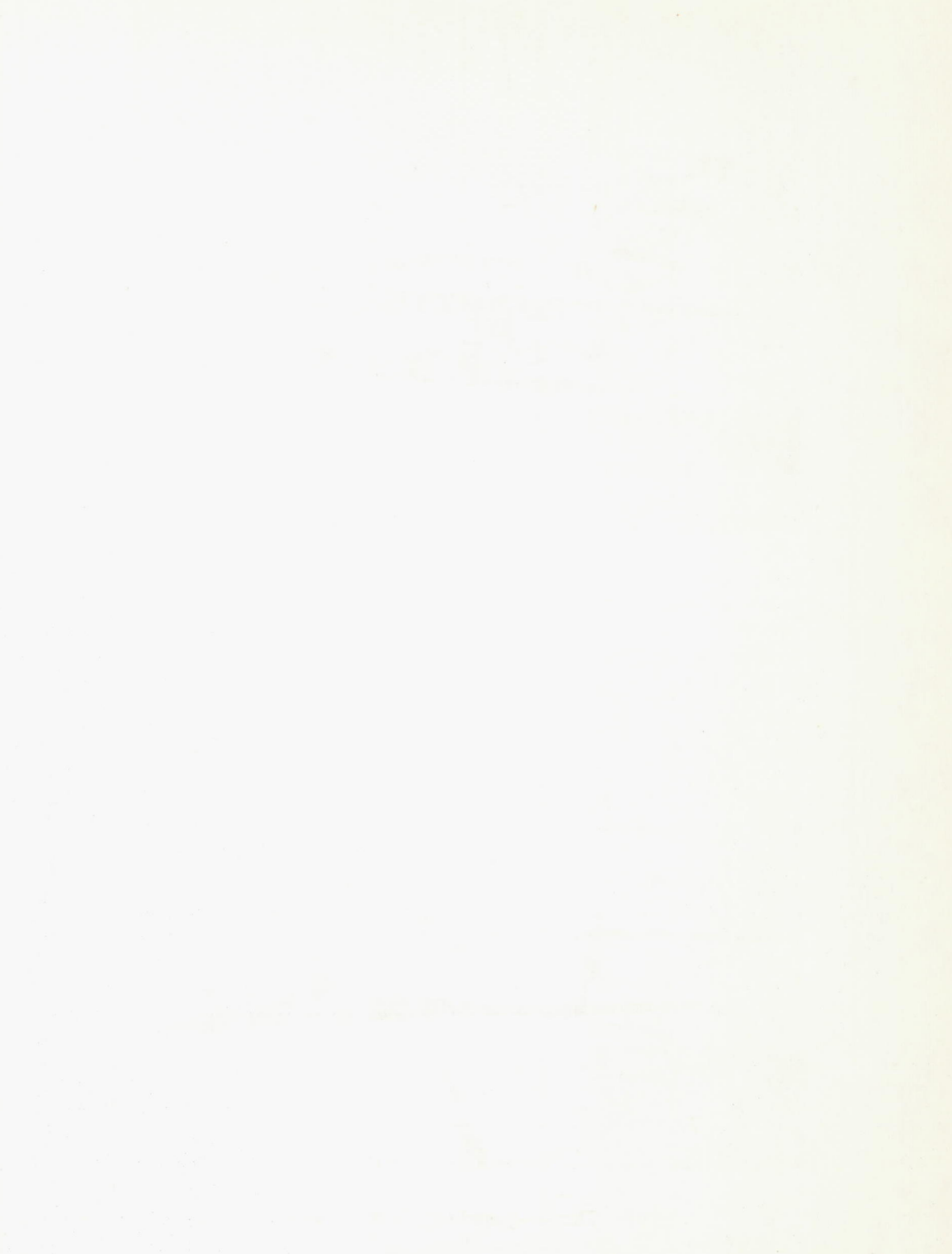
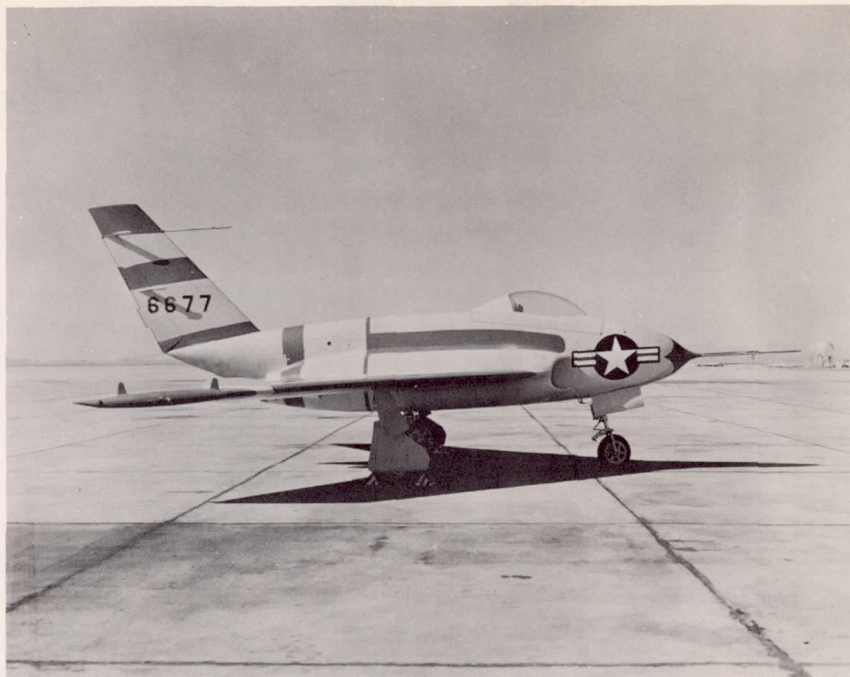
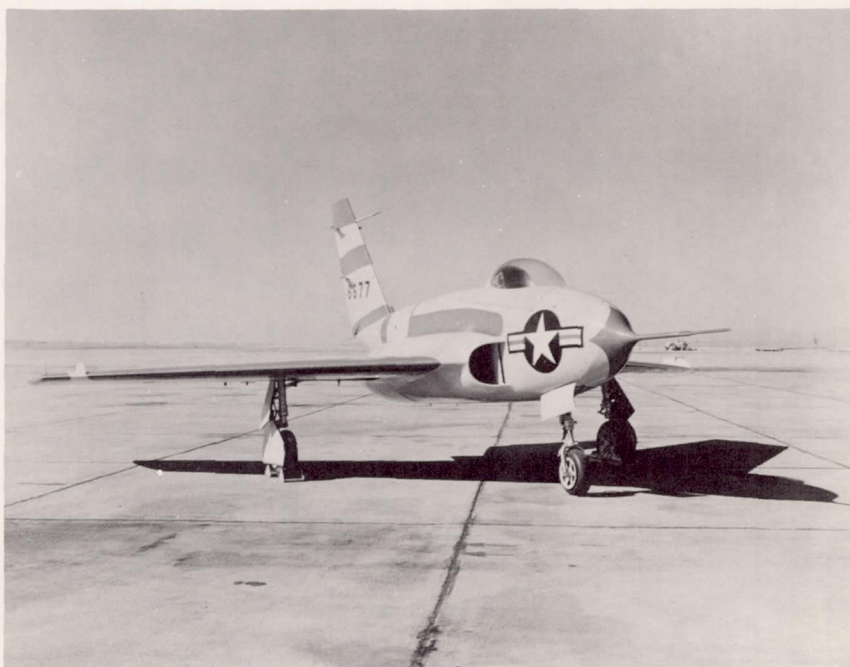


PLATE 12



(a) Side view.

NACA  
A-15116



(b) Three-quarter front view.

NACA  
A-15117

Figure 2.- The X-4 No. 2 airplane.



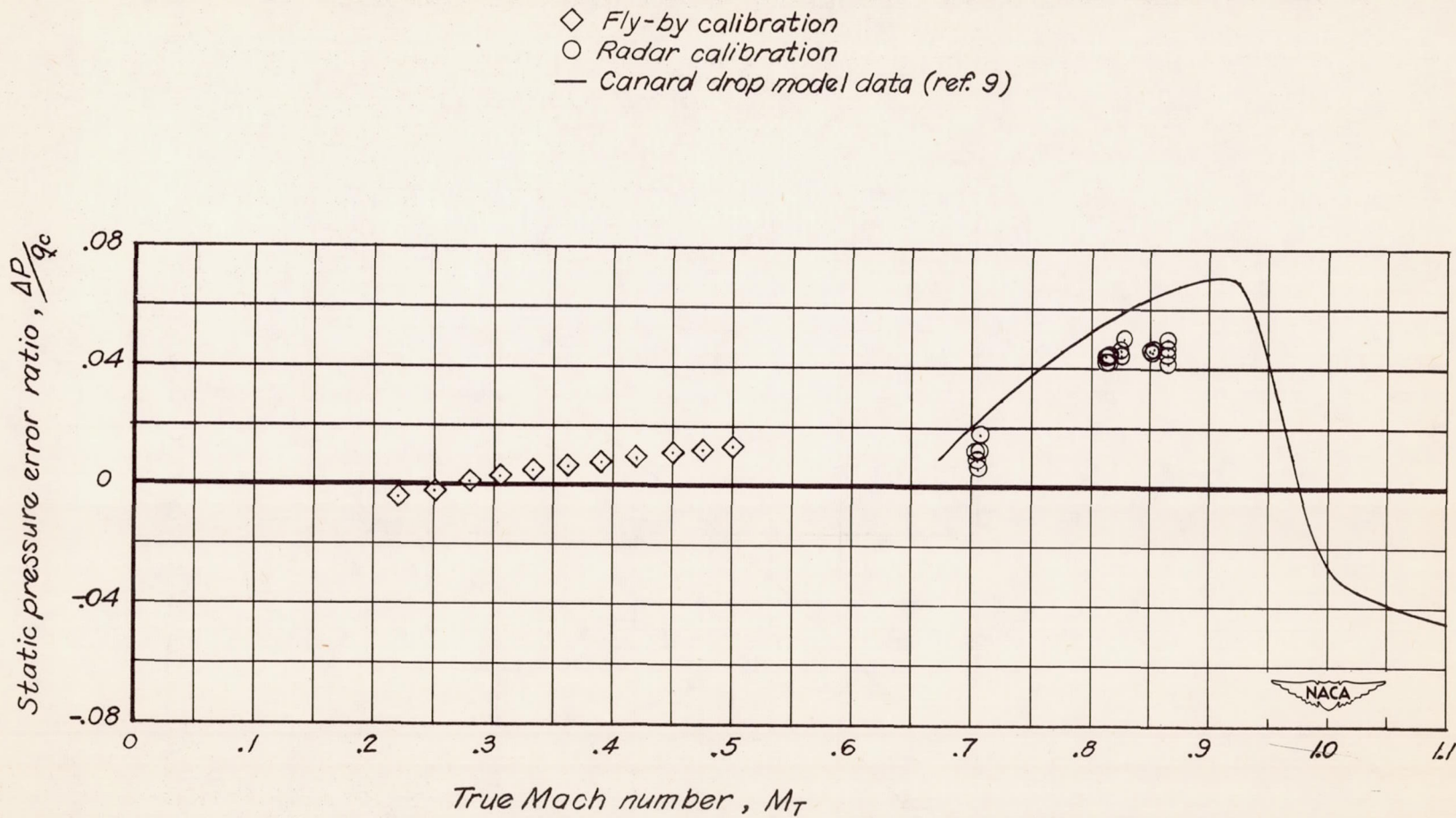


Figure 3.— Variation of the static pressure error ratio with Mach number in straight flight, X-4 airplane.

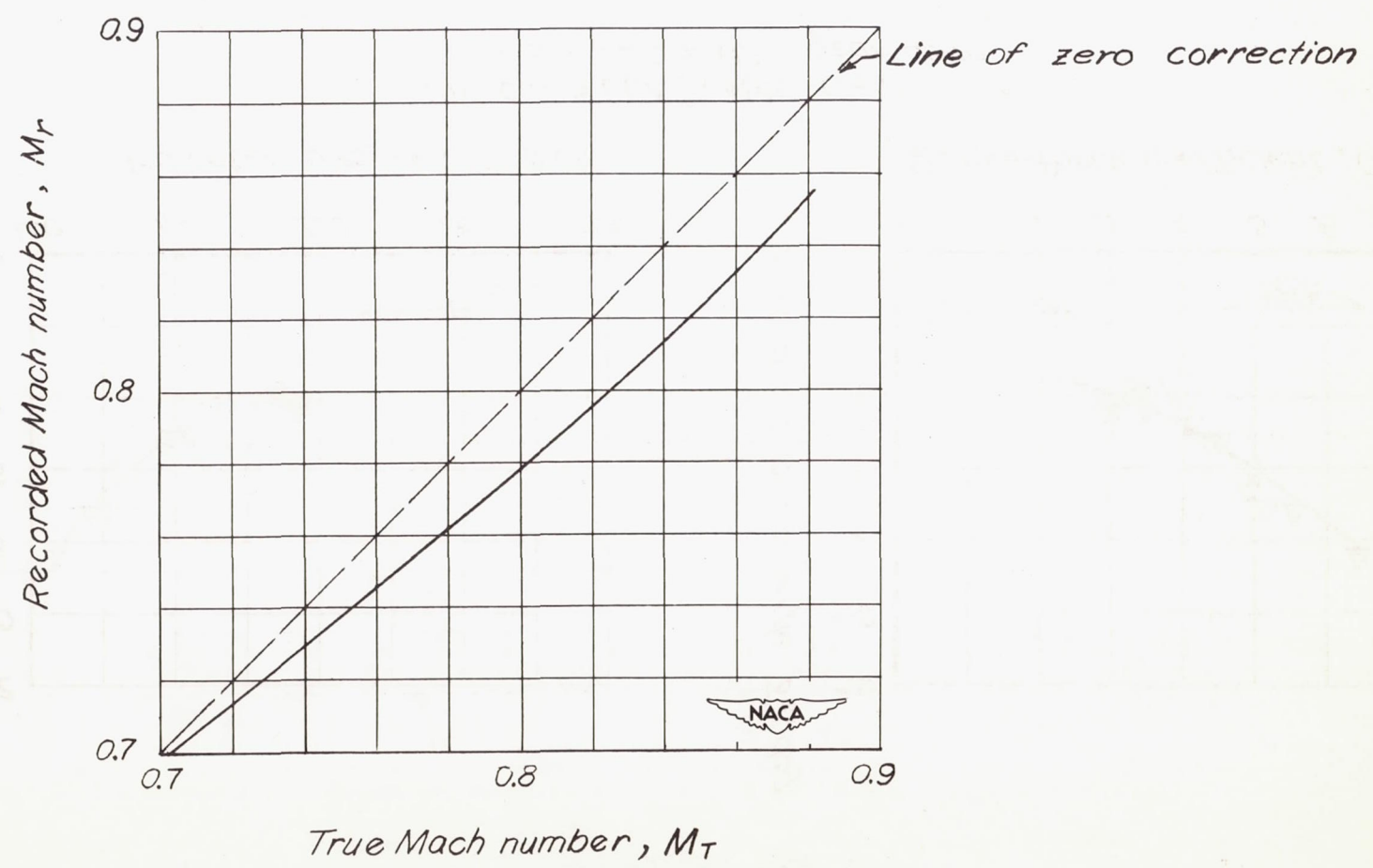


Figure 4.- Variation of true Mach number with recorded Mach number. X-4 airplane.



Configuration

Altitude

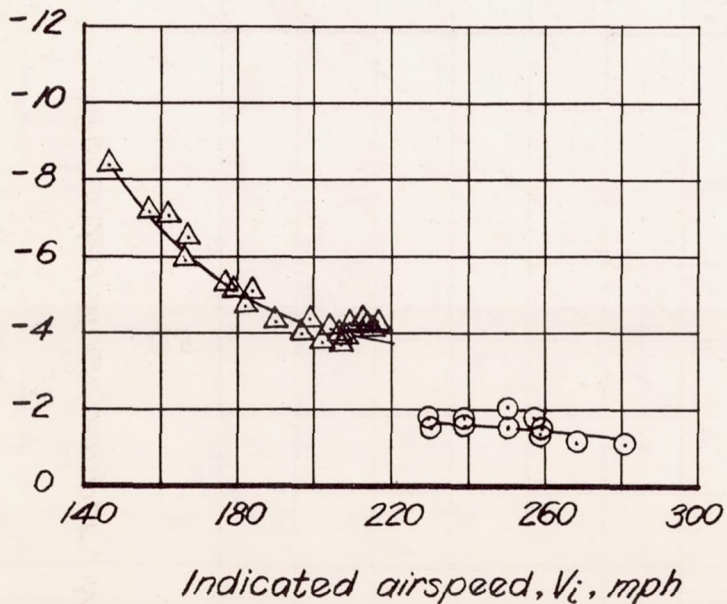
○ Clean

11,000 feet

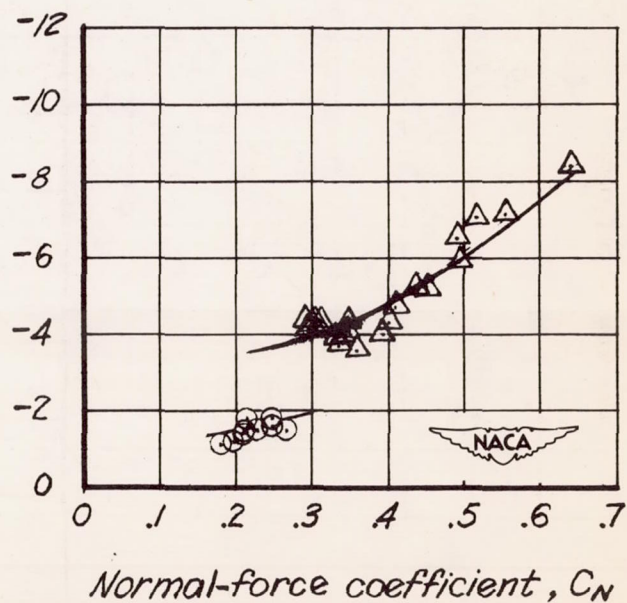
△ Gear down, flaps up

2,200 feet

Longitudinal control angle,  $\delta_e$ , deg.



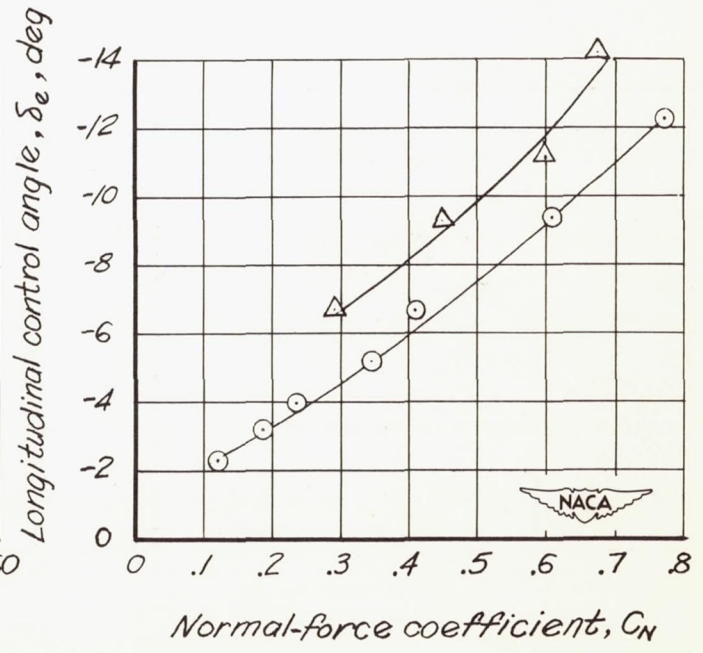
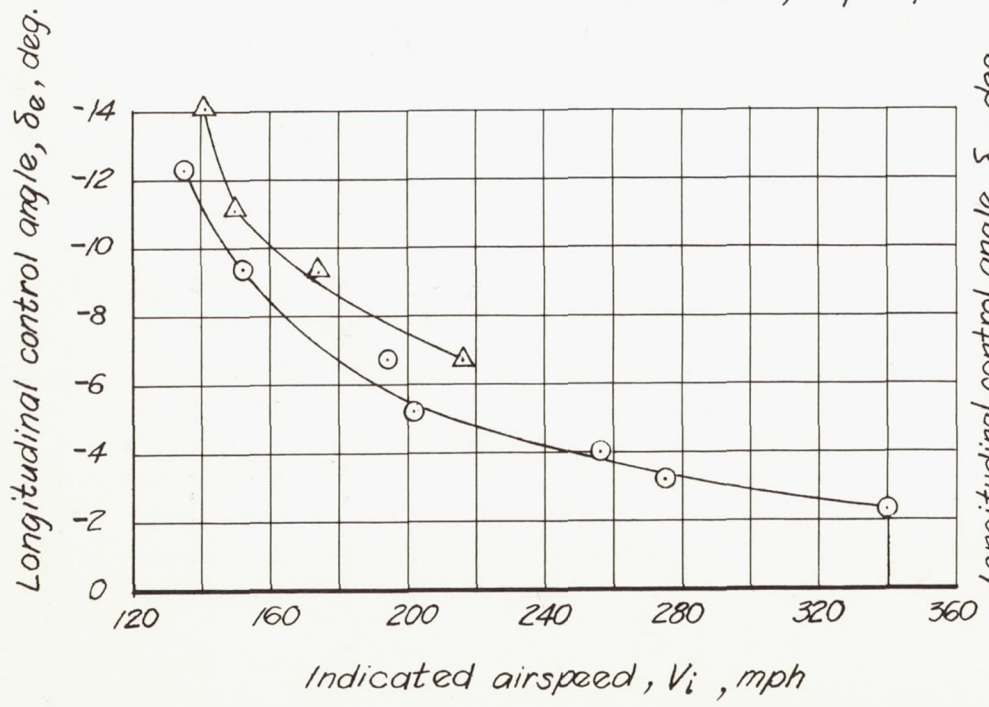
Longitudinal control angle,  $\delta_e$ , deg.



(a) c.g.  $\approx$  21.4 % MAC clean.  
 c.g.  $\approx$  22.0 % MAC gear down.

Figure 5.- Longitudinal stability characteristics in straight flight of the X-4 airplane.

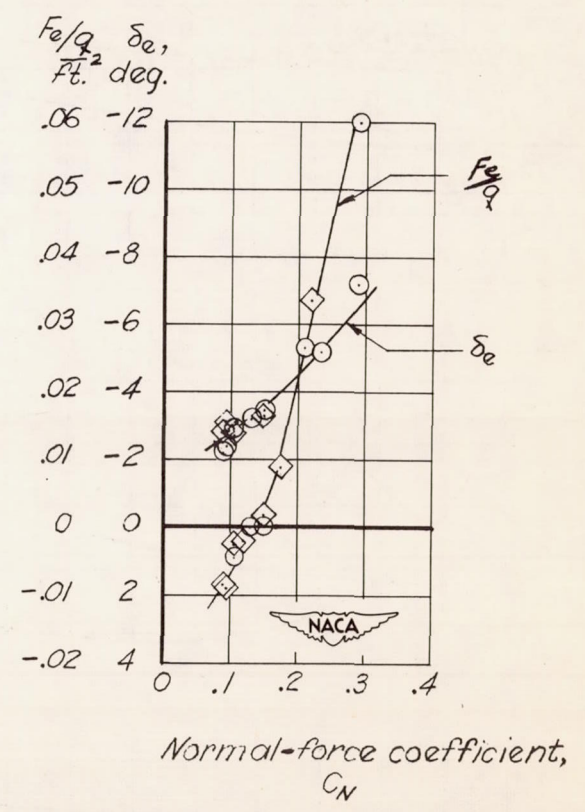
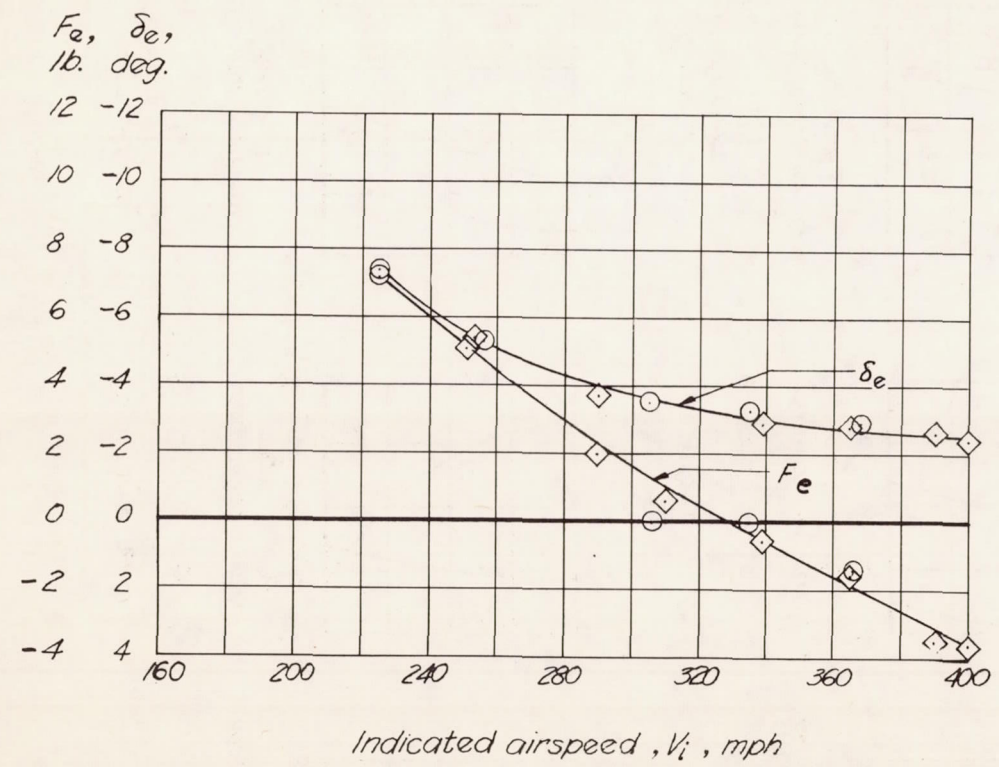
<i>Configuration</i>	<i>Altitude</i>
○ <i>Clean</i>	15,000 feet
△ <i>Gear down, flaps up</i>	15,000 feet



(b) c.g.  $\approx$  19.5 % MAC

Figure 5.- Continued.

Configuration                      Altitude  
 ○ Clean                              15,000 feet  
 ◇ Clean                              10,000 feet



(C) c.g.  $\approx$  18.0% MAC

Figure 5.- Concluded.

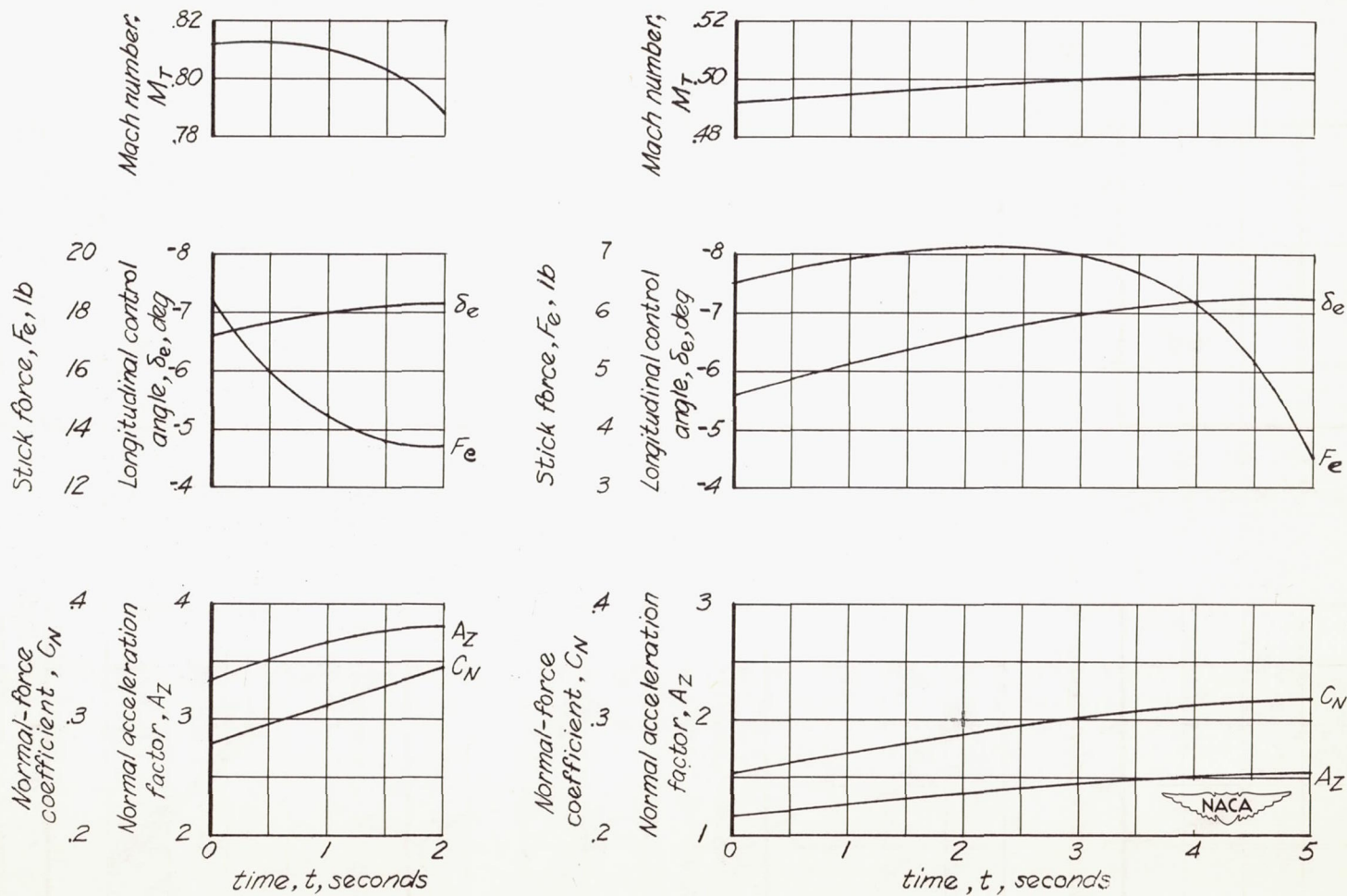
(a)  $h_p = 20,700$  feet;  $c.g. \approx 18.4\%$  MAC.(b)  $h_p = 20,000$  feet;  $c.g. \approx 17.8\%$  MAC.

Figure 6.— Time histories of pertinent variables obtained during typical accelerated stability runs. X-4 airplane.

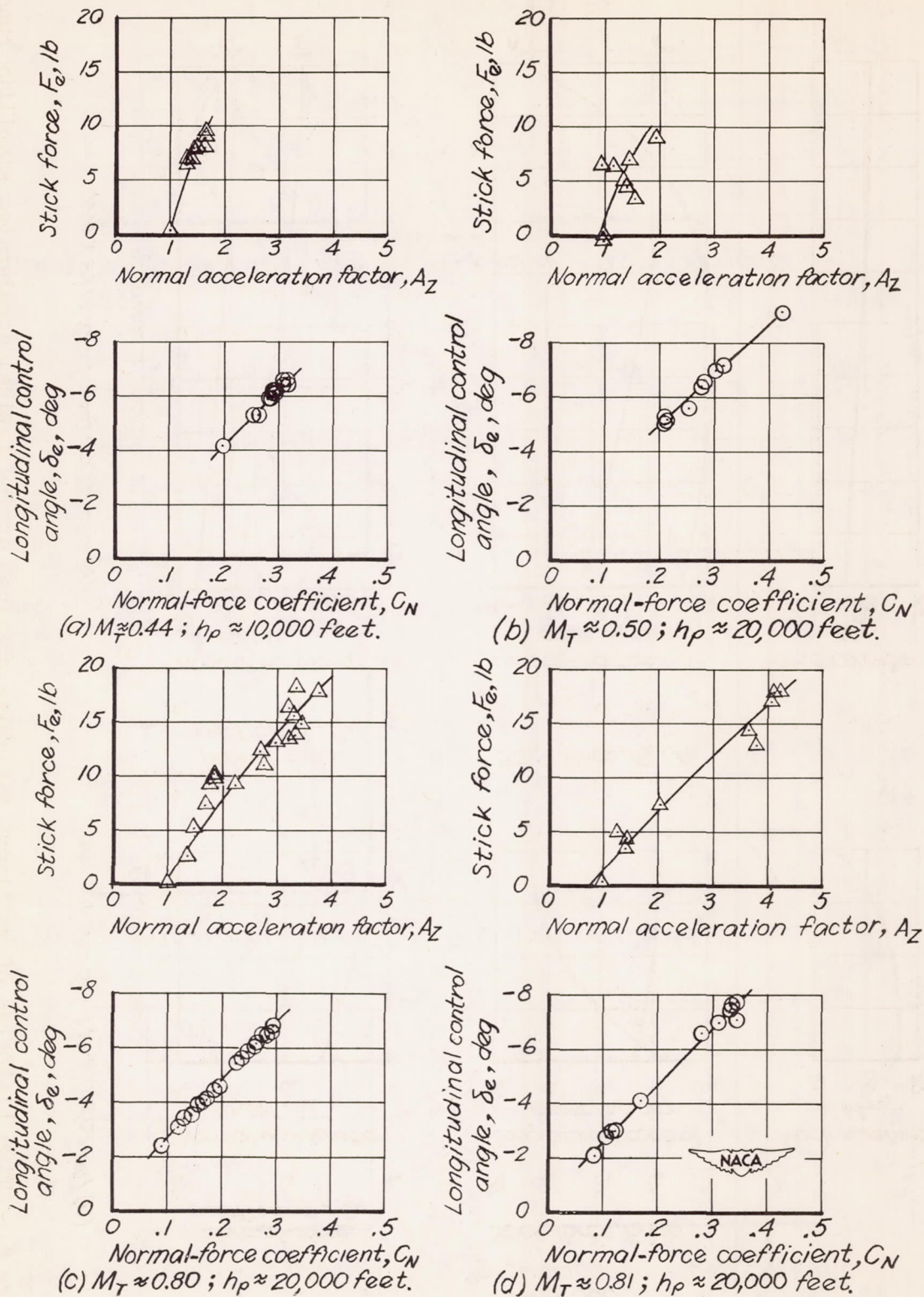


Figure 7.— Variation of elevator control angle and control force with normal-force coefficient for several values of Mach number. X-4 airplane.

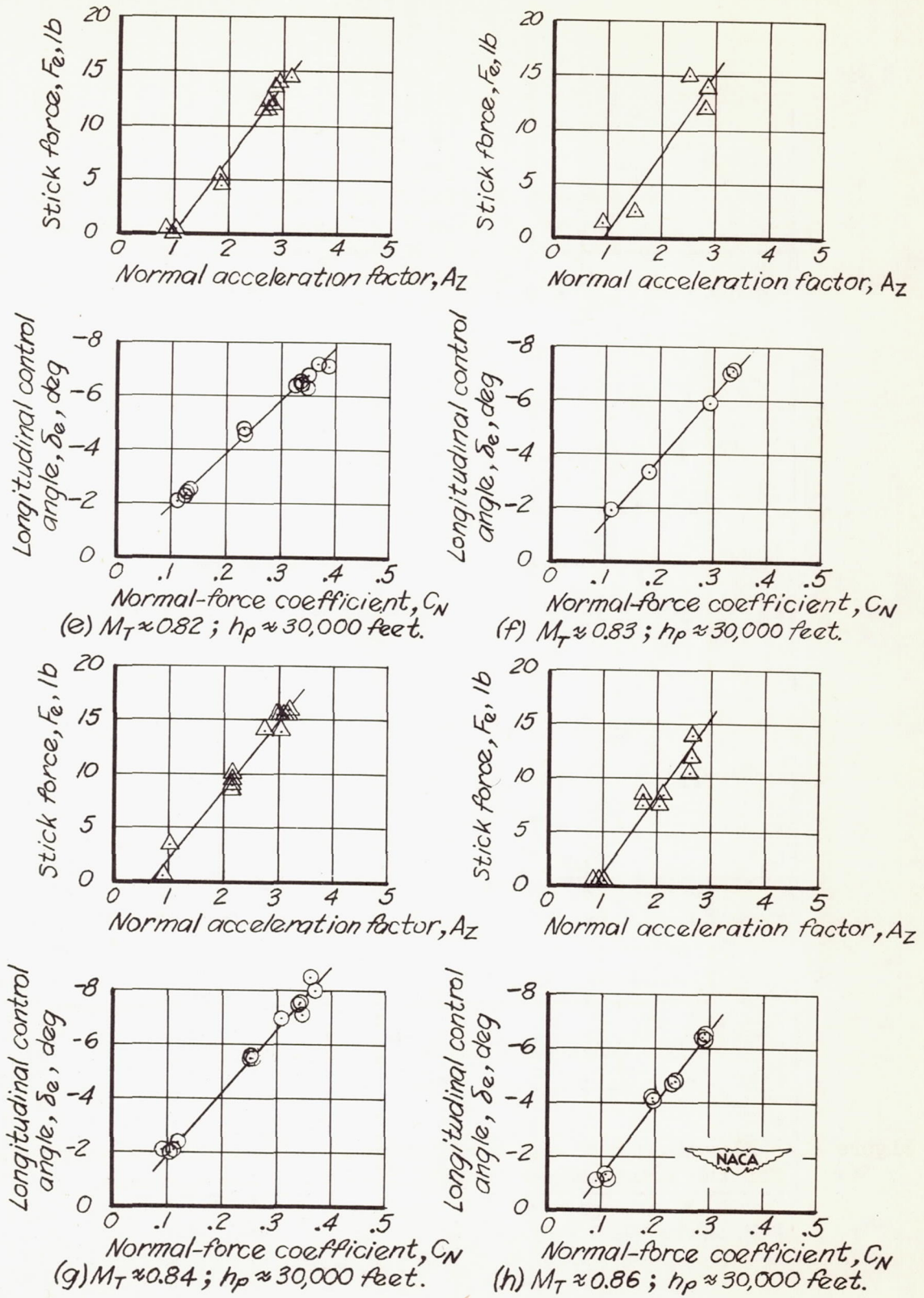


Figure 7.- Concluded.

- △ Flight 15, Run 7;  $M \approx 0.82$ ;  $h_p = 20,000$  feet
- Flight 18, Run 7;  $M \approx 0.82$ ;  $h_p = 30,000$  feet
- Flight 18, Run 6;  $M \approx 0.82$ ; Do.
- ◇ Flight 19, Run 9;  $M \approx 0.82$ ; Do.
- △ Flight 19, Run 17;  $M \approx 0.84$ ; Do.

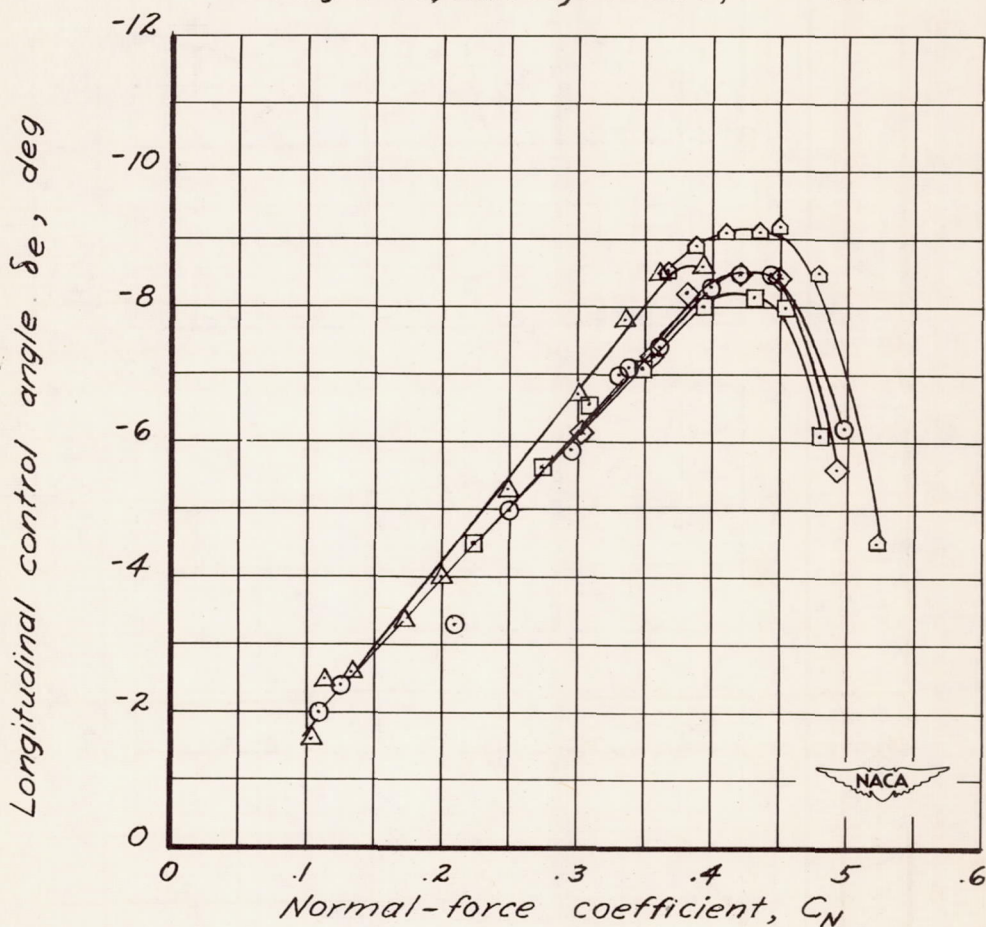


Figure 8.- Elevon-control-angle variation with normal-force coefficient for the longitudinal instability runs. X-4 airplane.

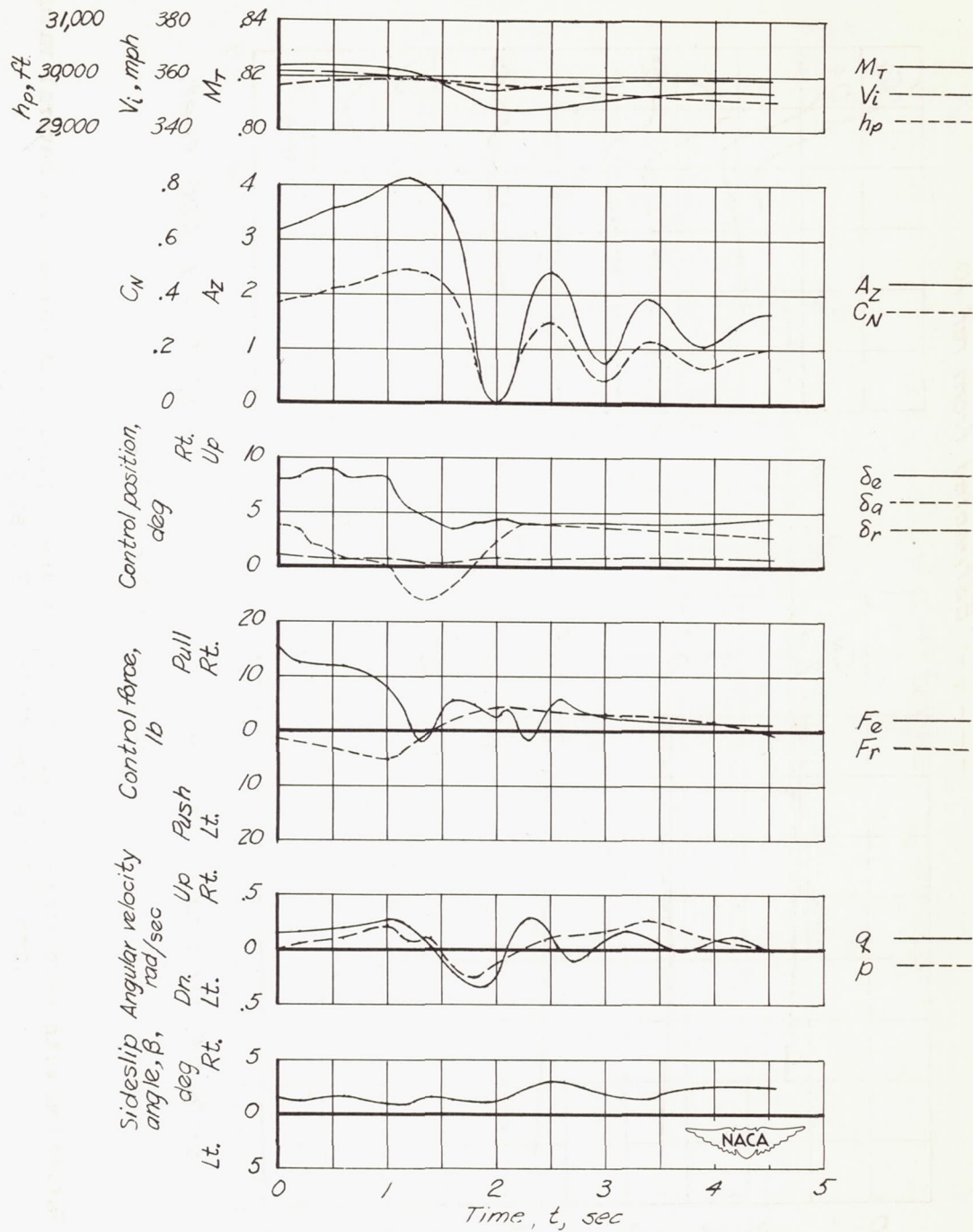


Figure 9.— Time history of longitudinal instability encountered at a Mach number of 0.82 and a normal-force coefficient of about 0.42. X-4 airplane.



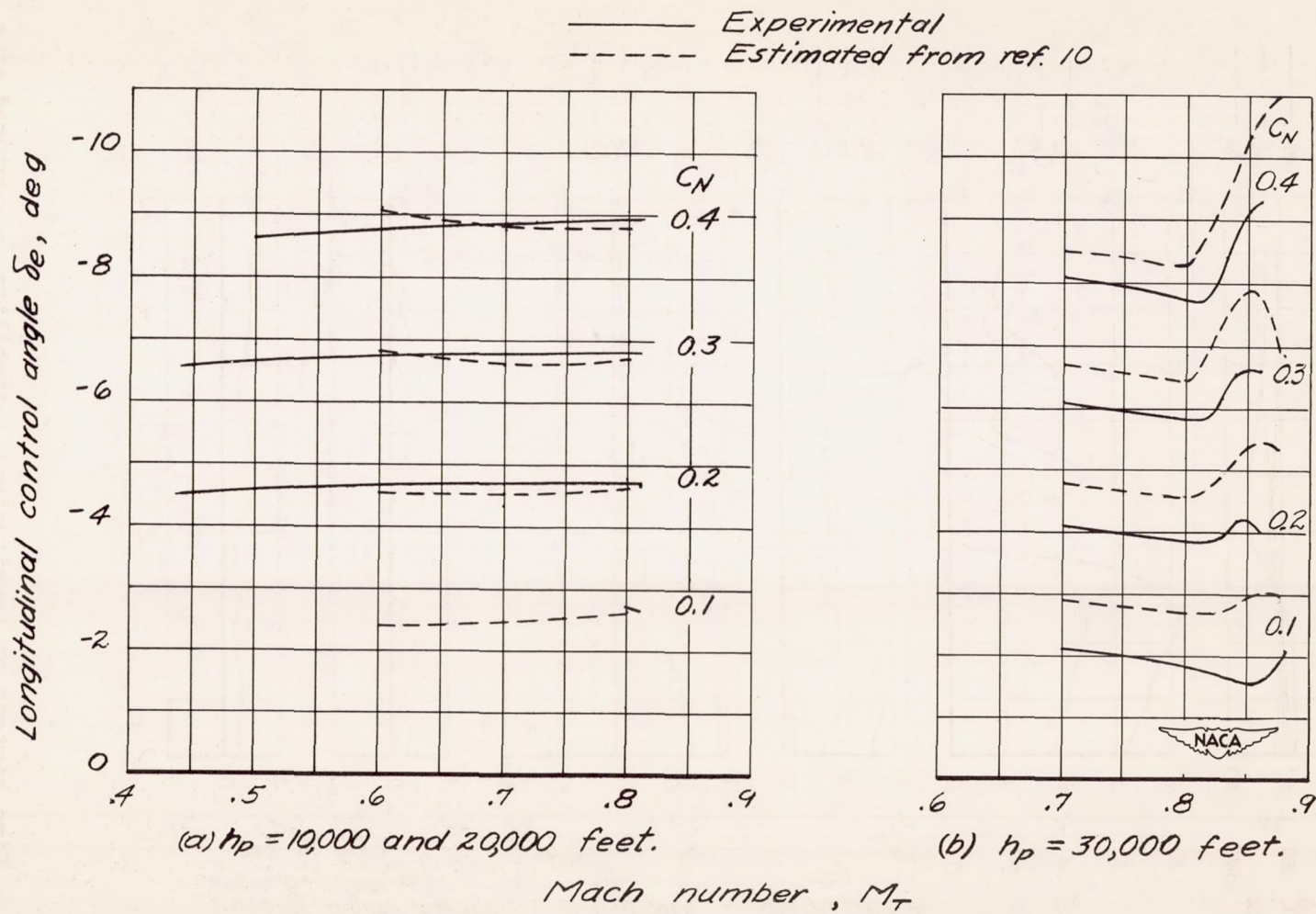


Figure 10.— Variation with Mach number of the elevon angles required for balance at several values of normal-force coefficient. X-4 airplane.

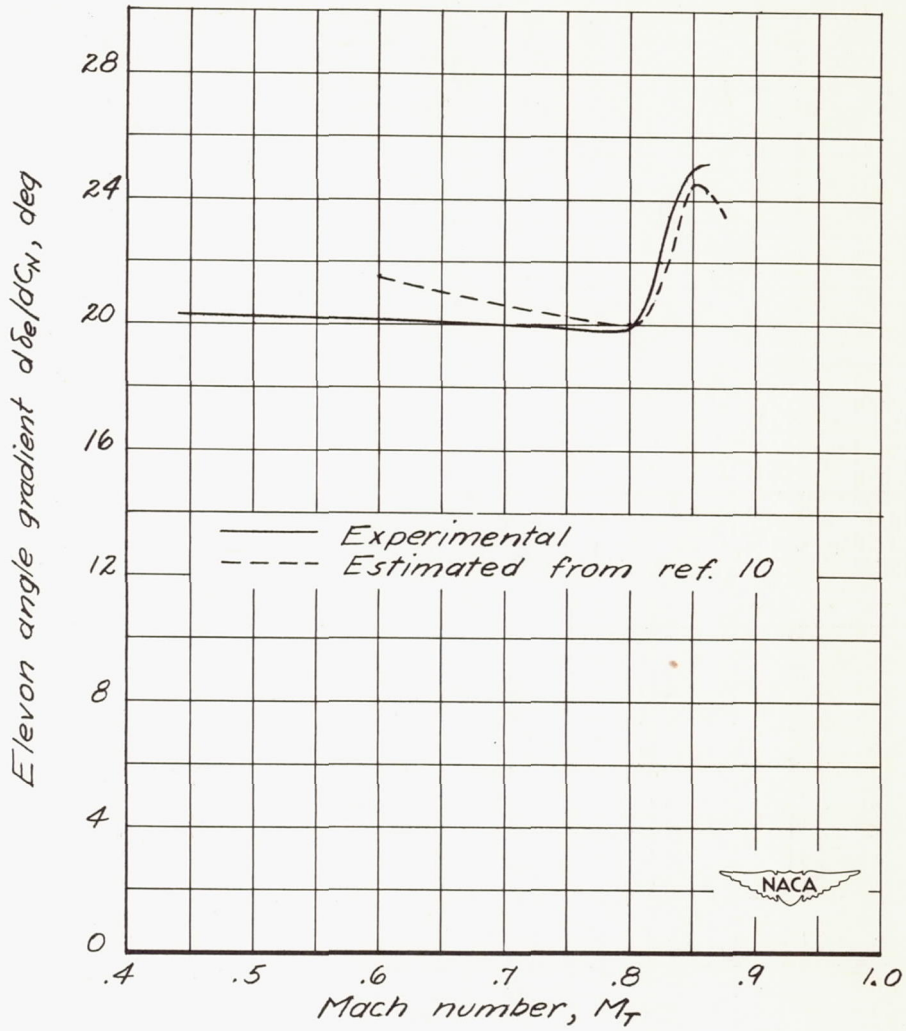
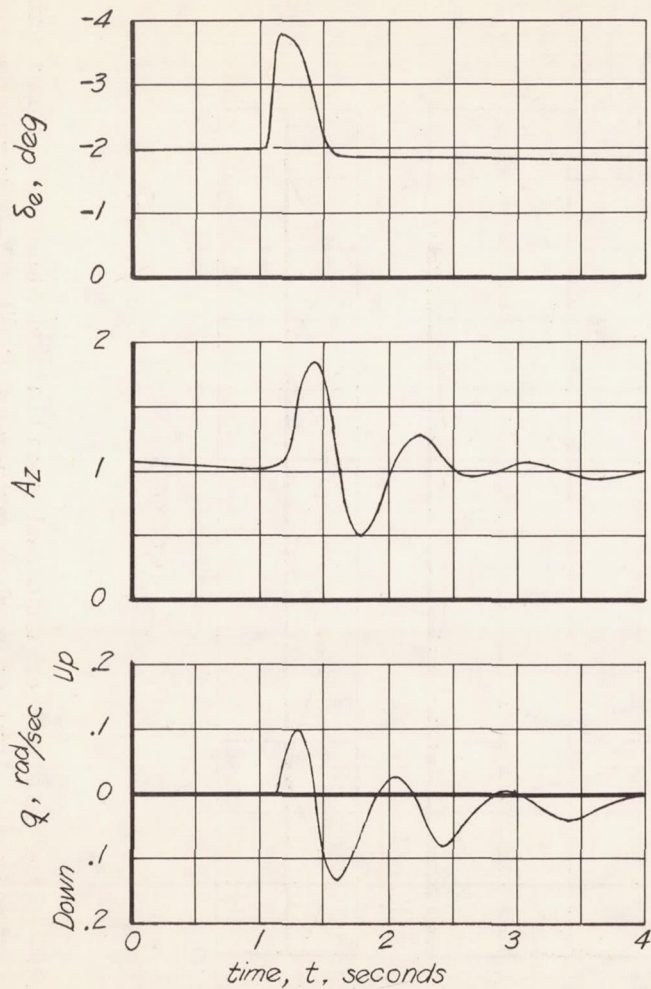
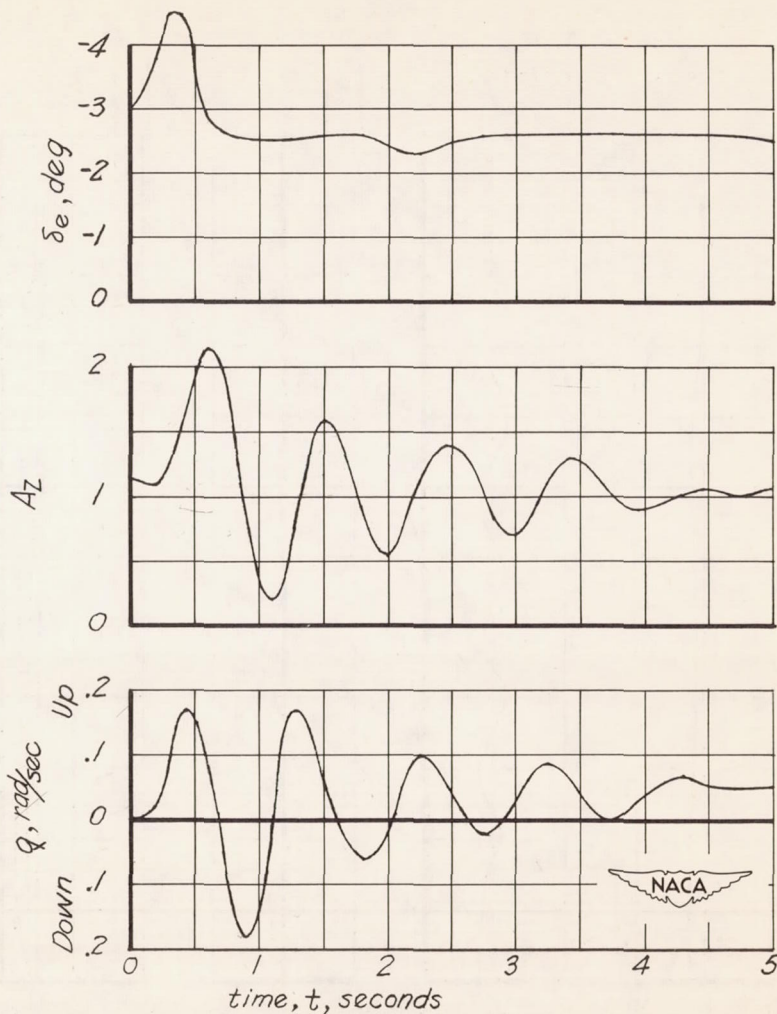


Figure 11.— Variation of the elevon-angle gradient with Mach number.  
X-4 airplane.



(a)  $h_p \approx 20,000$  feet.



(b)  $h_p \approx 30,000$  feet.

Figure 12.- Typical time histories of pilot-excited longitudinal oscillations of X-4 airplane.

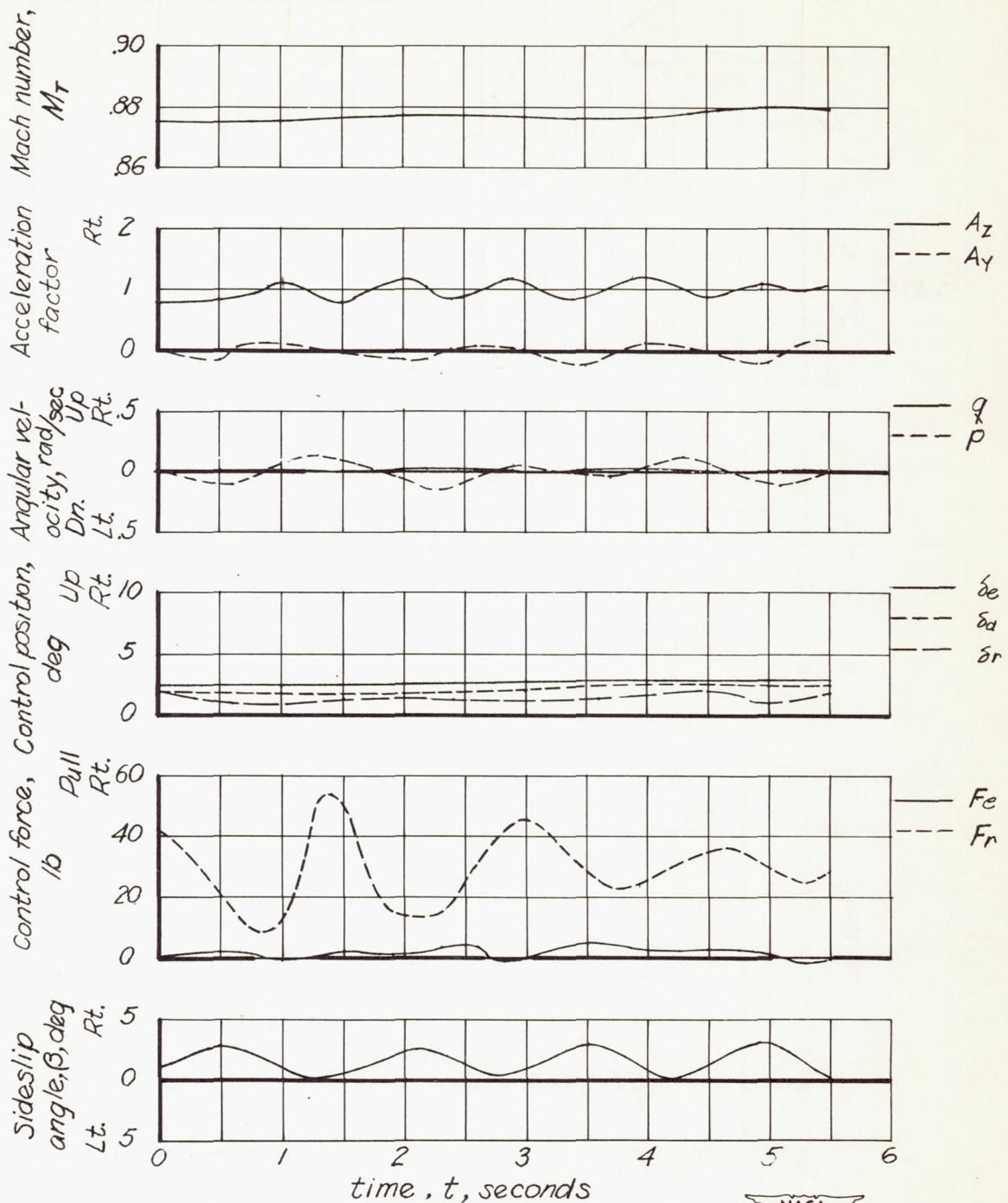


Figure 13.- Time history of undamped oscillation about all three axes in straight flight at a Mach number of 0.88. X-4 airplane.

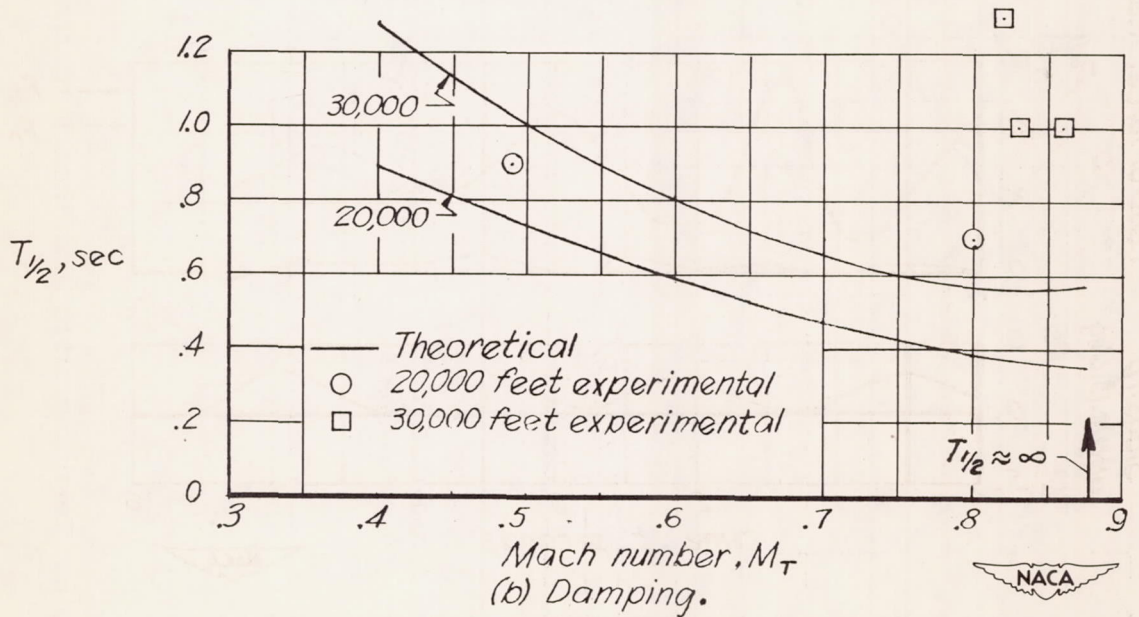
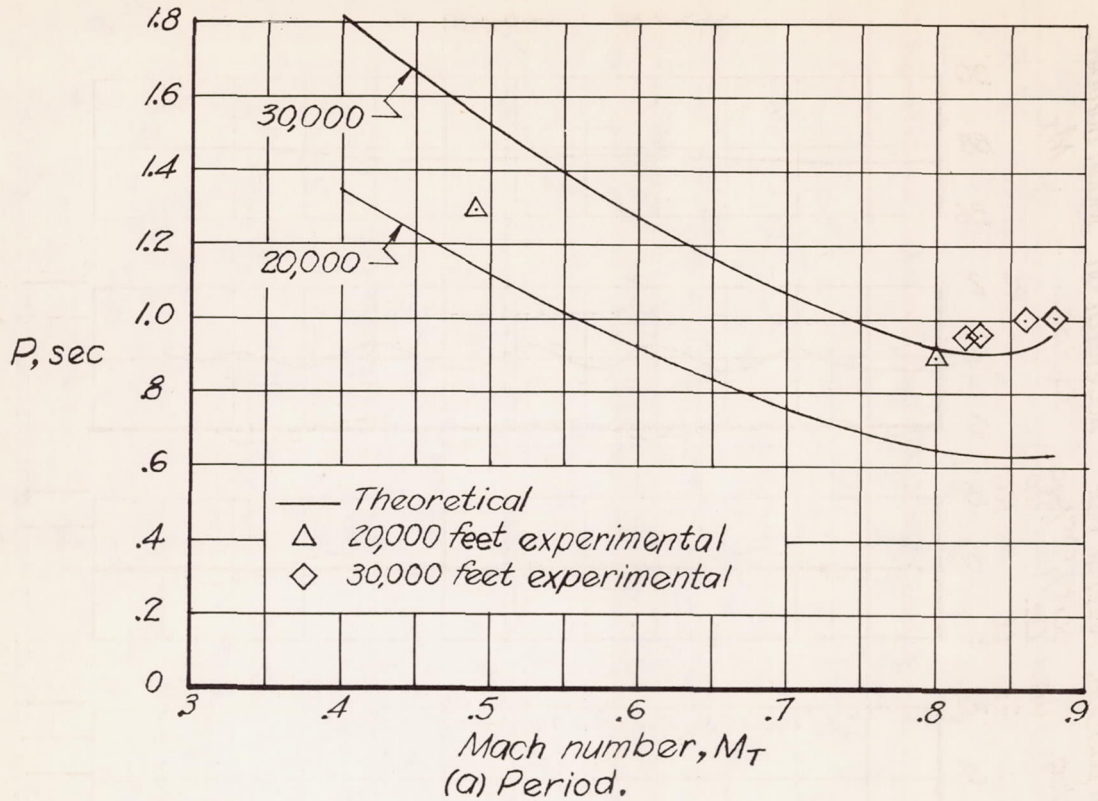
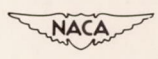
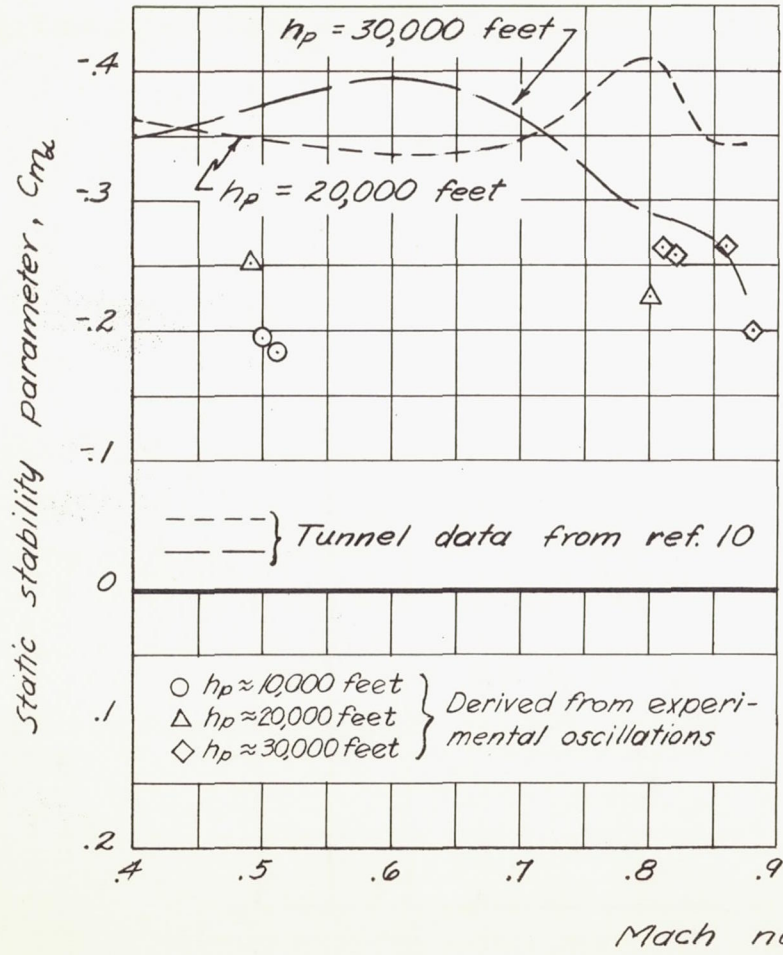
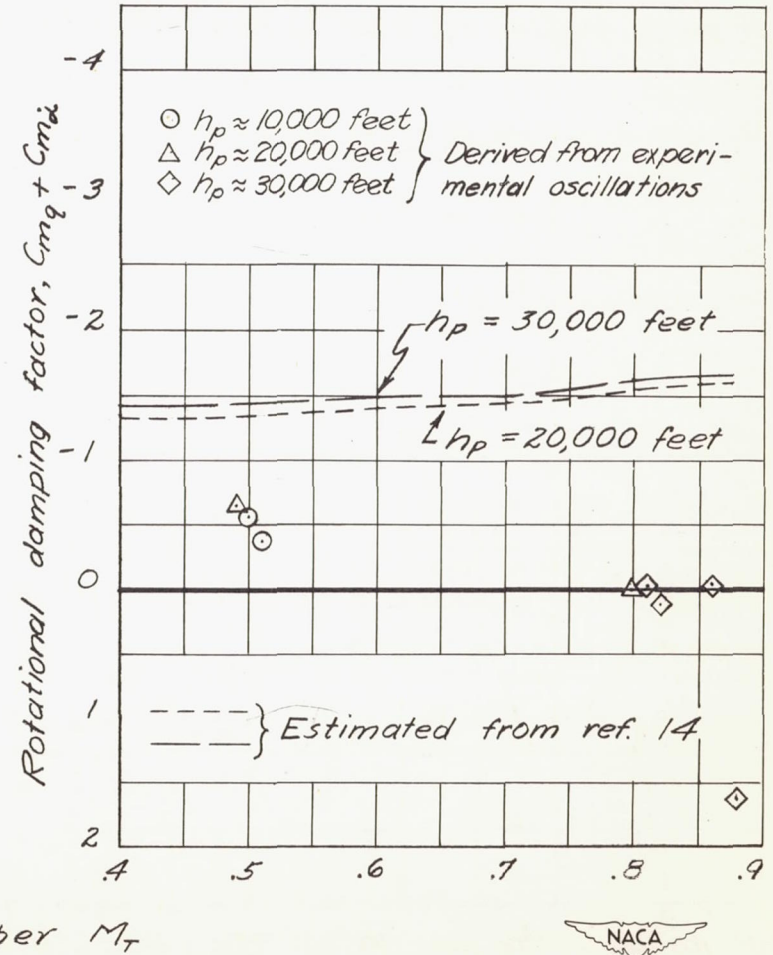


Figure 14.— Comparison of the experimental short-period longitudinal oscillation period and damping with values computed by the simplified theory. X-4 airplane.





(a)  $C_{m\alpha}$



(b)  $C_{mq} + C_{m\dot{\alpha}}$



Figure 15.- Variation with Mach number of the static stability and rotational damping derivatives. X-4 airplane.

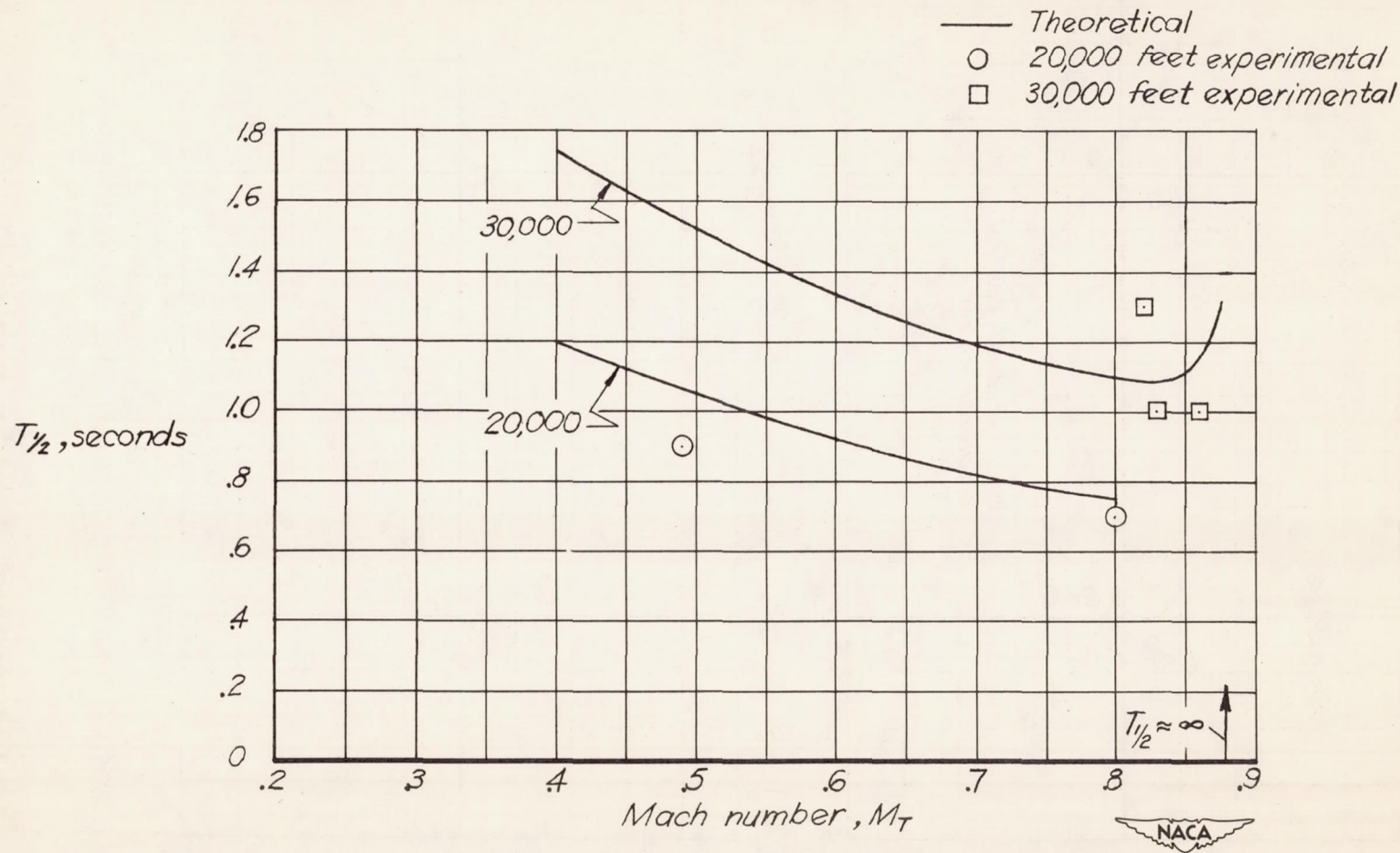


Figure 16.— Comparison of the experimental damping with values computed using the derived values of rotational damping factor. X-4 airplane.

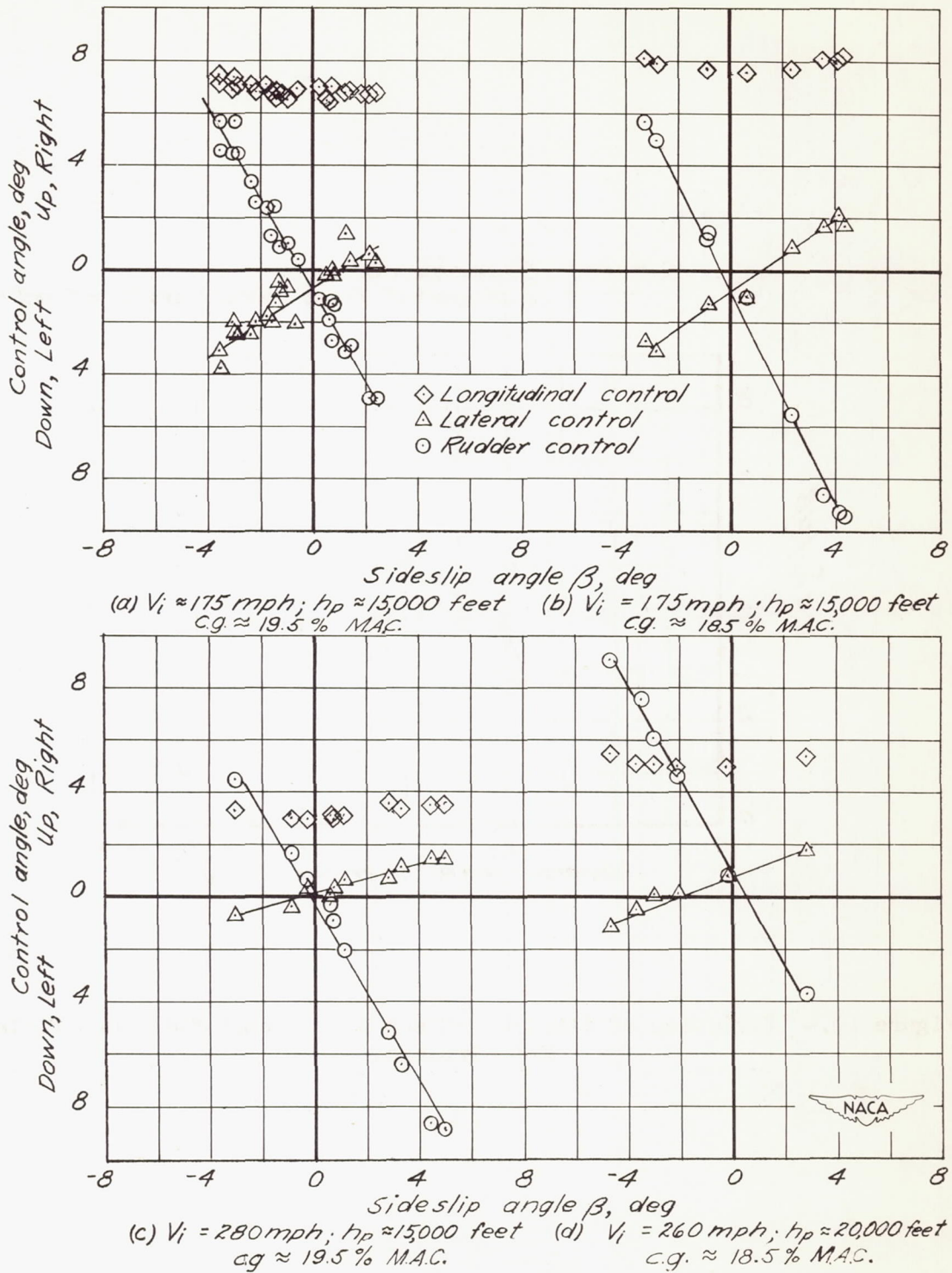


Figure 17.— Lateral and directional stability characteristics of X-4 airplane in steady sideslips at several values of indicated airspeed and pressure altitude.



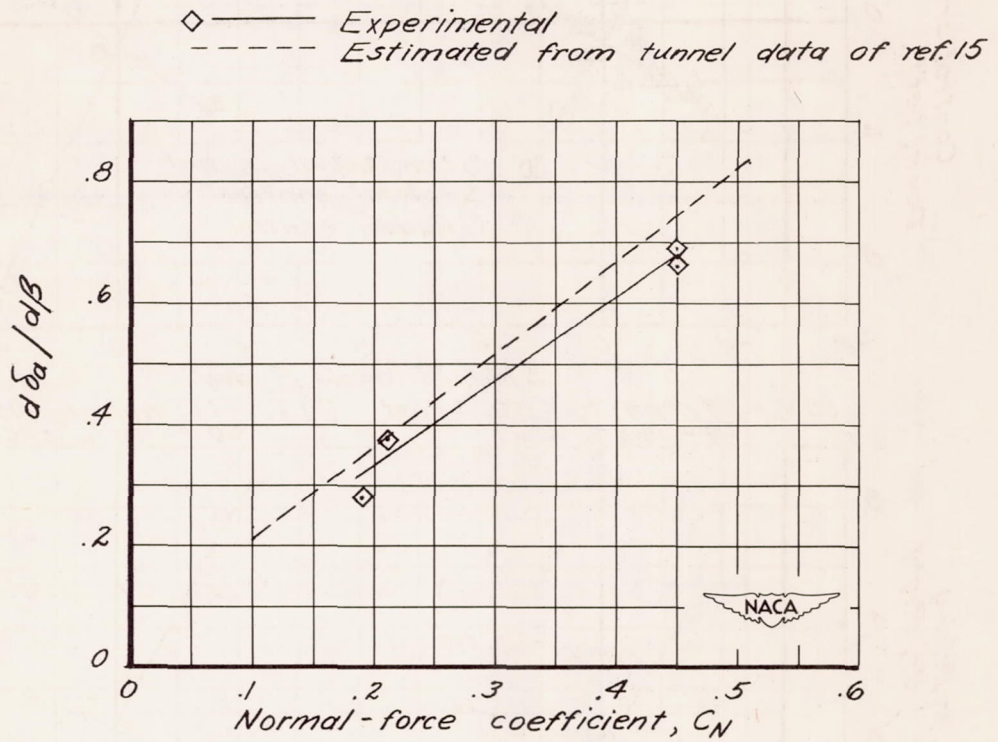
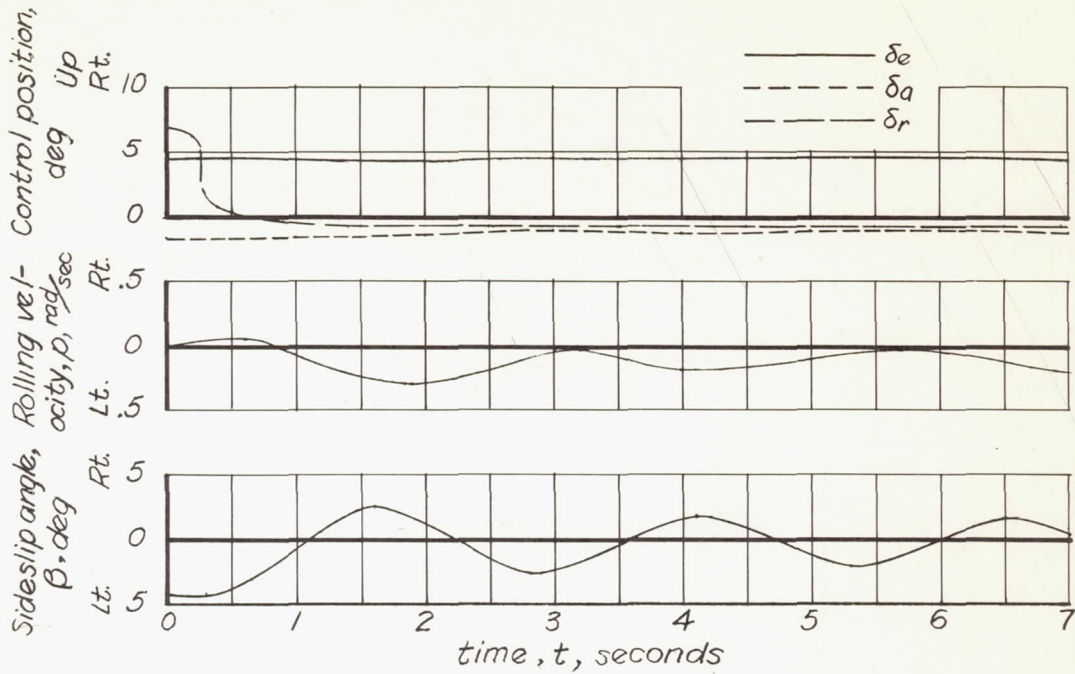
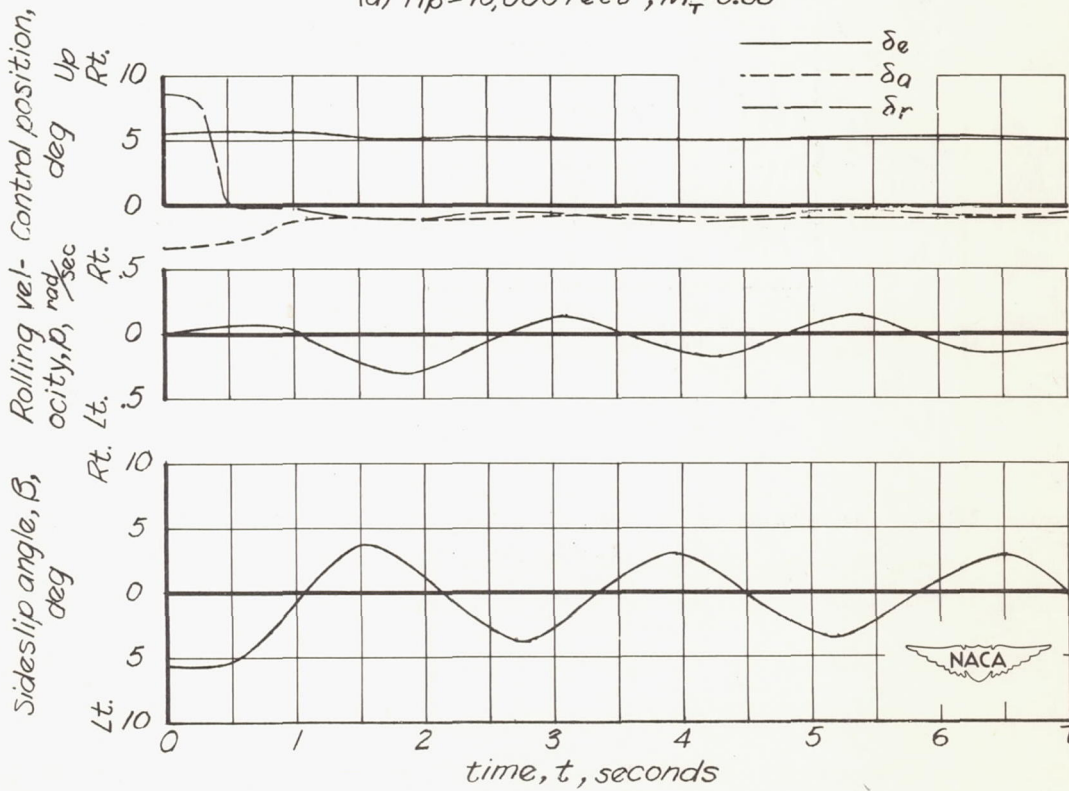


Figure 18.— Variation of dihedral effect with normal-force coefficient.  
 X-4 airplane.



(a)  $h_p = 10,000$  feet ;  $M_T \approx 0.35$



(b)  $h_p = 30,000$  feet ;  $M_T \approx 0.51$ .

Figure 19.— Time histories of typical lateral oscillations of X-4 airplane.

- Computed; 30,000 feet
- Computed; 10,000 feet
- Experimental; 30,000 feet
- ◇ Experimental; 10,000 feet
- △ Experimental; 10,000 feet; gear down

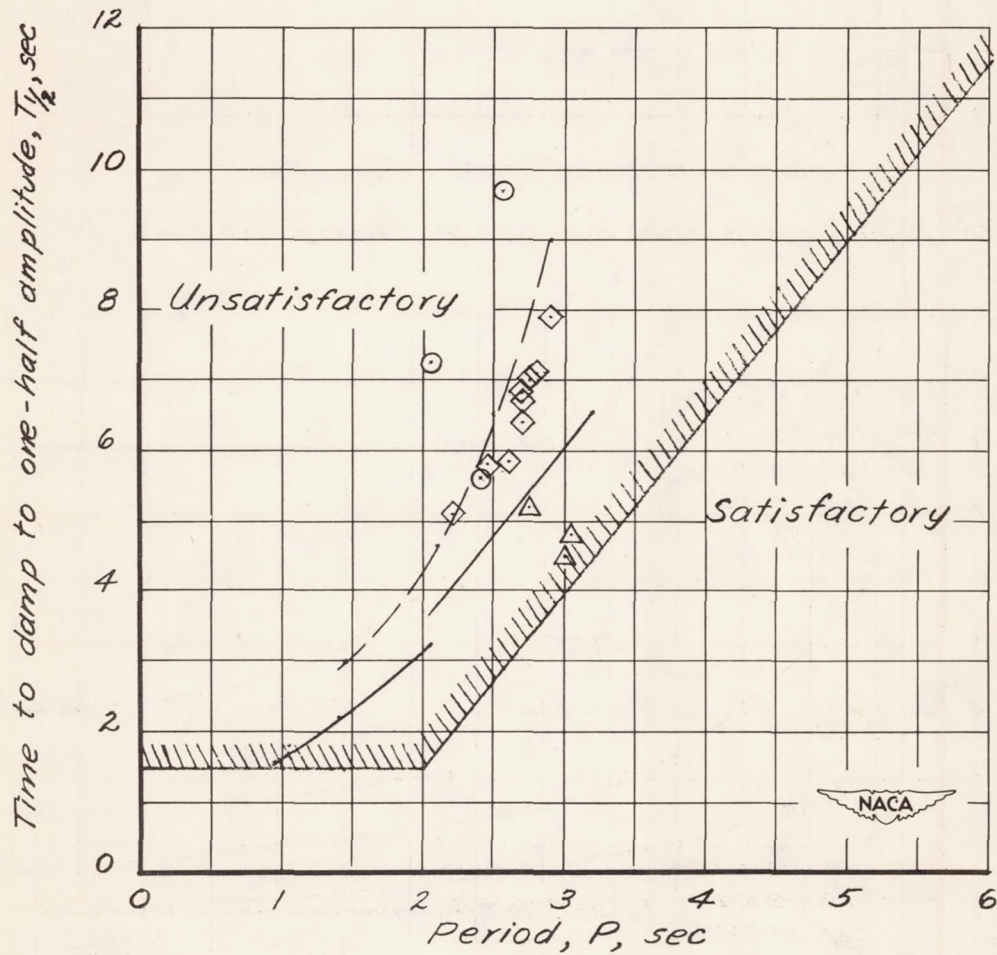
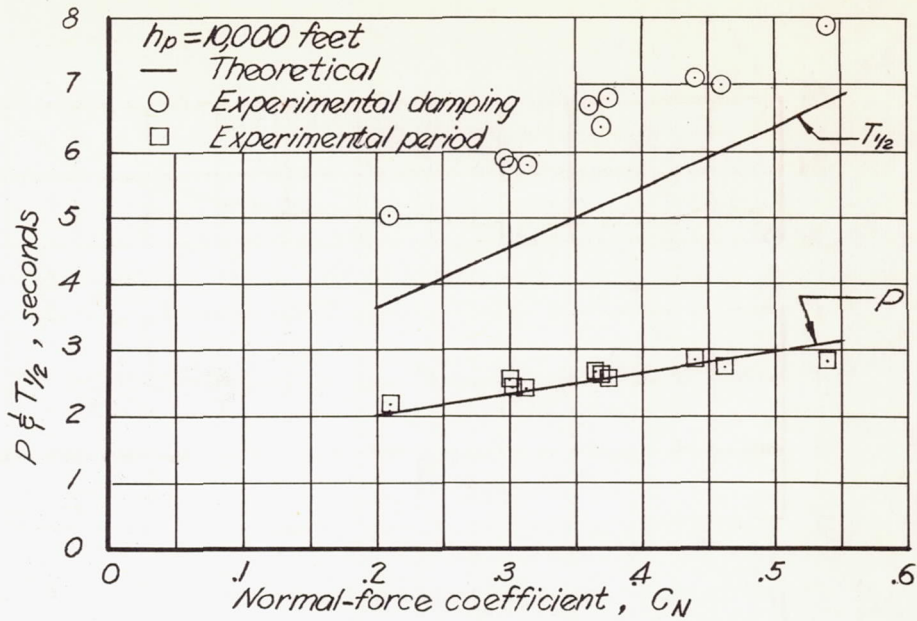
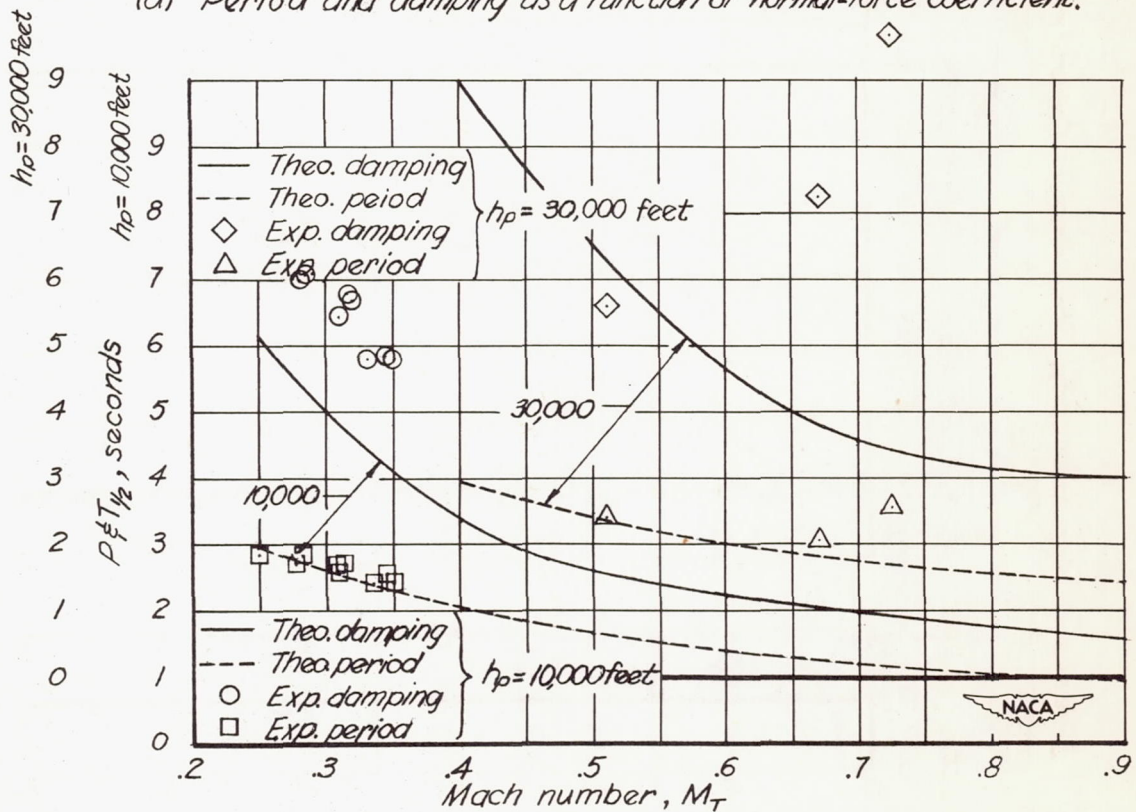


Figure 20.— Comparison between dynamic lateral stability of X-4 airplane and the criterion for satisfactory characteristics.



(a) Period and damping as a function of normal-force coefficient.



(b) Period and damping as a function of Mach number.

Figure 21.— Period and damping lateral dynamic stability characteristics of the X-4 airplane.

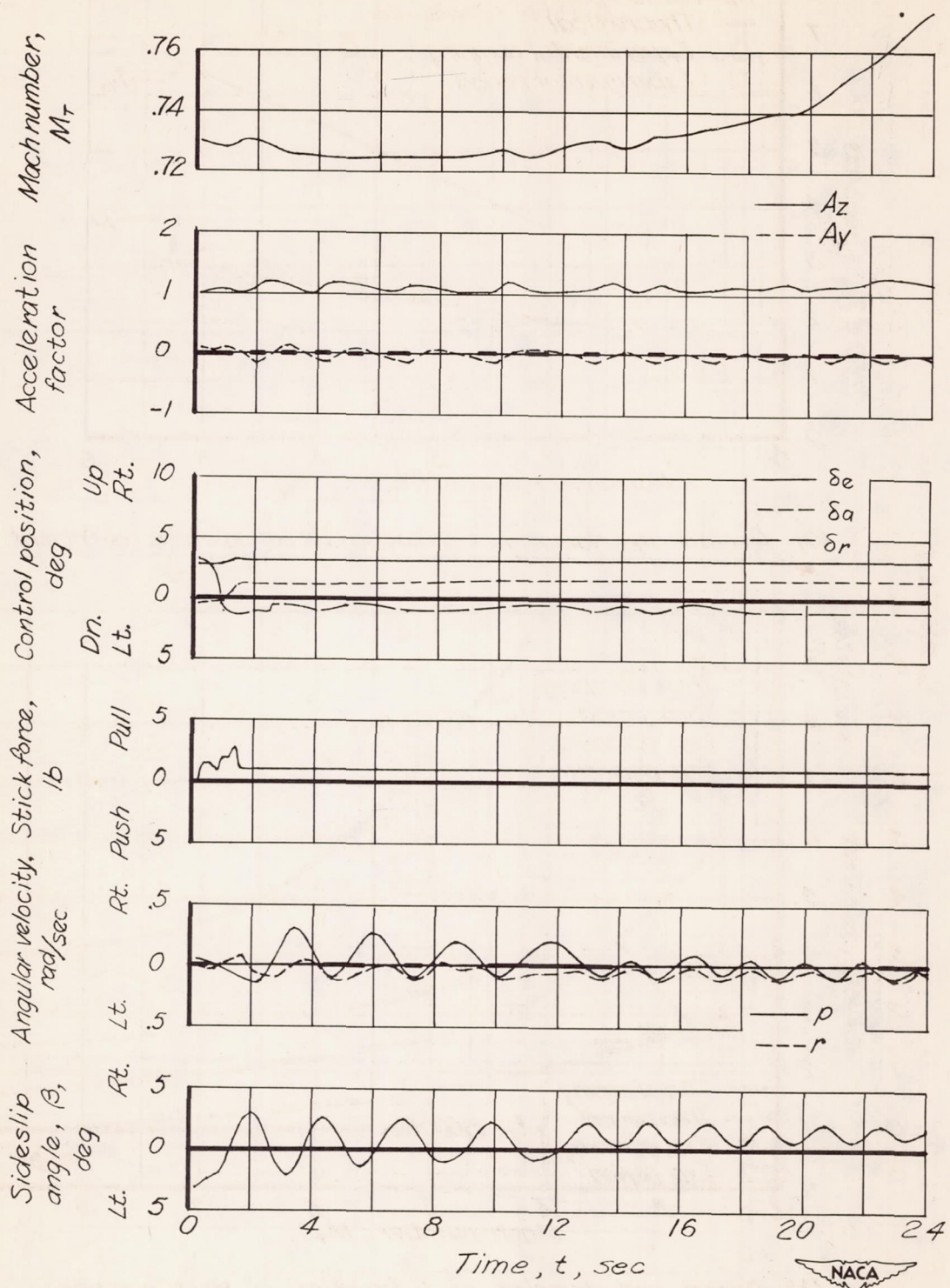


Figure 22.- Time history of unusual lateral oscillation experienced at a pressure altitude of 30,000 feet. X-4 airplane.

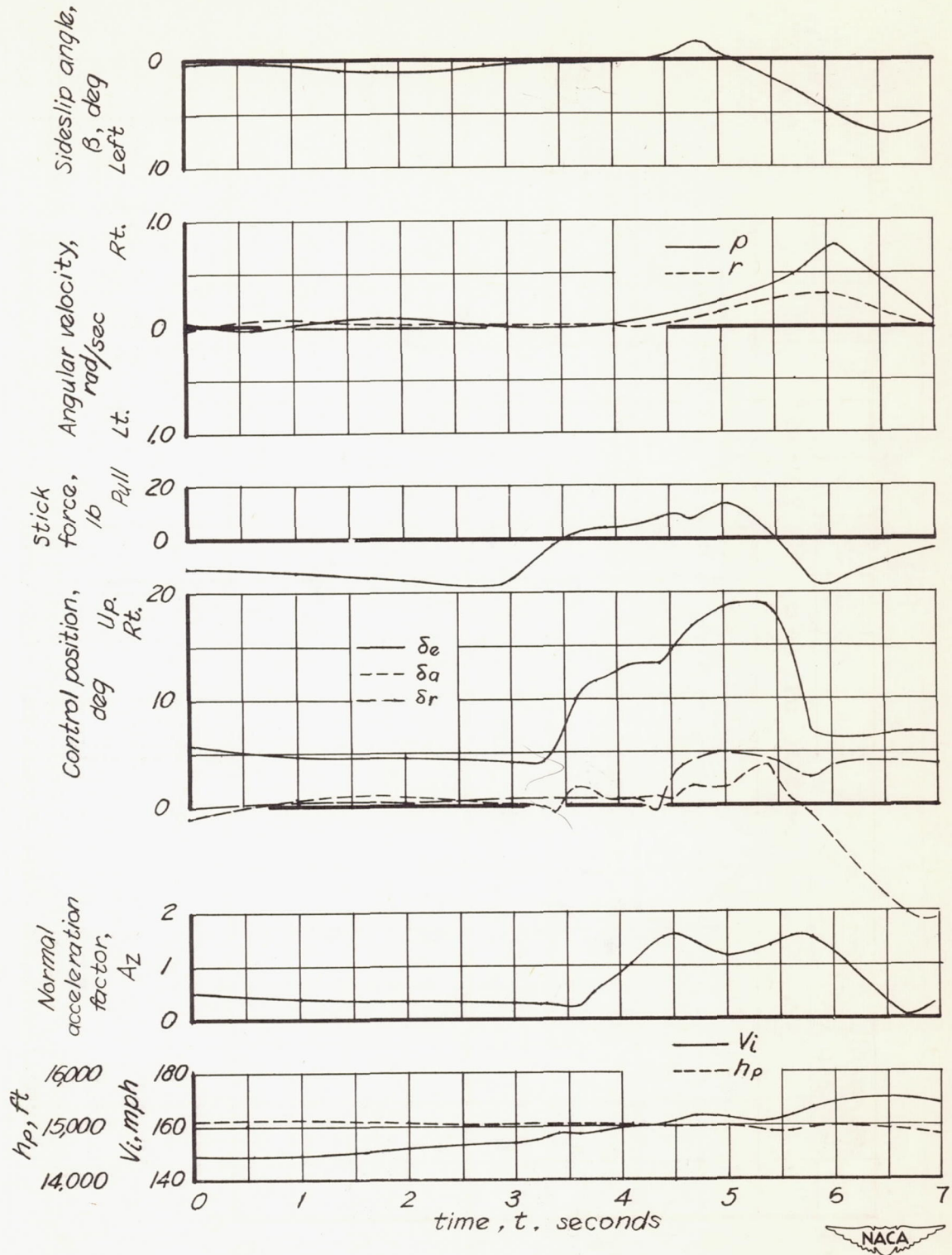


Figure 23.- Time history of a low-speed accelerated stall. X-4 airplane.

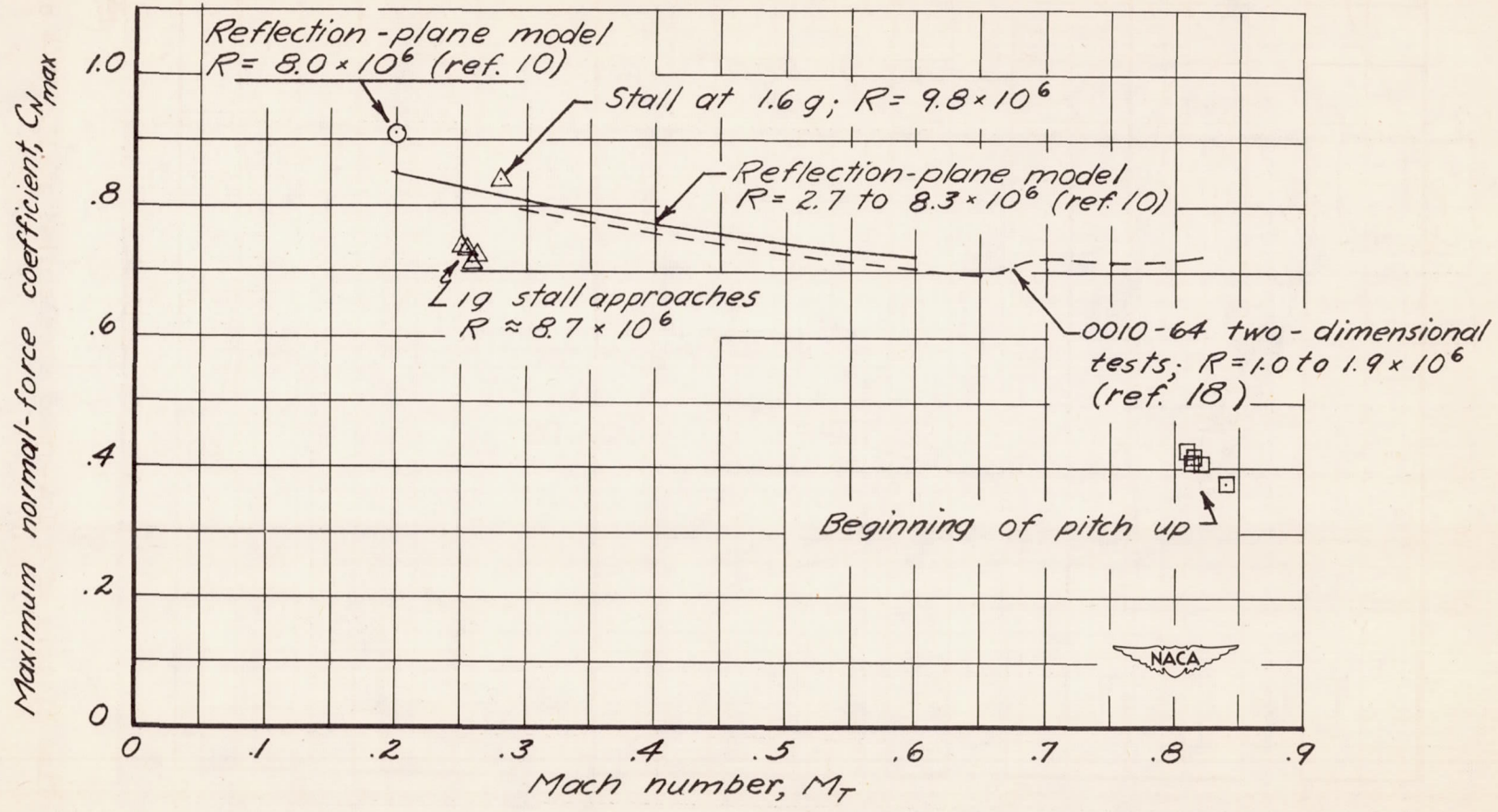


Figure 24.- Comparison of maximum lift coefficients measured in flight with values obtained from two-dimensional and three-dimensional wind-tunnel tests. X-4 airplane.

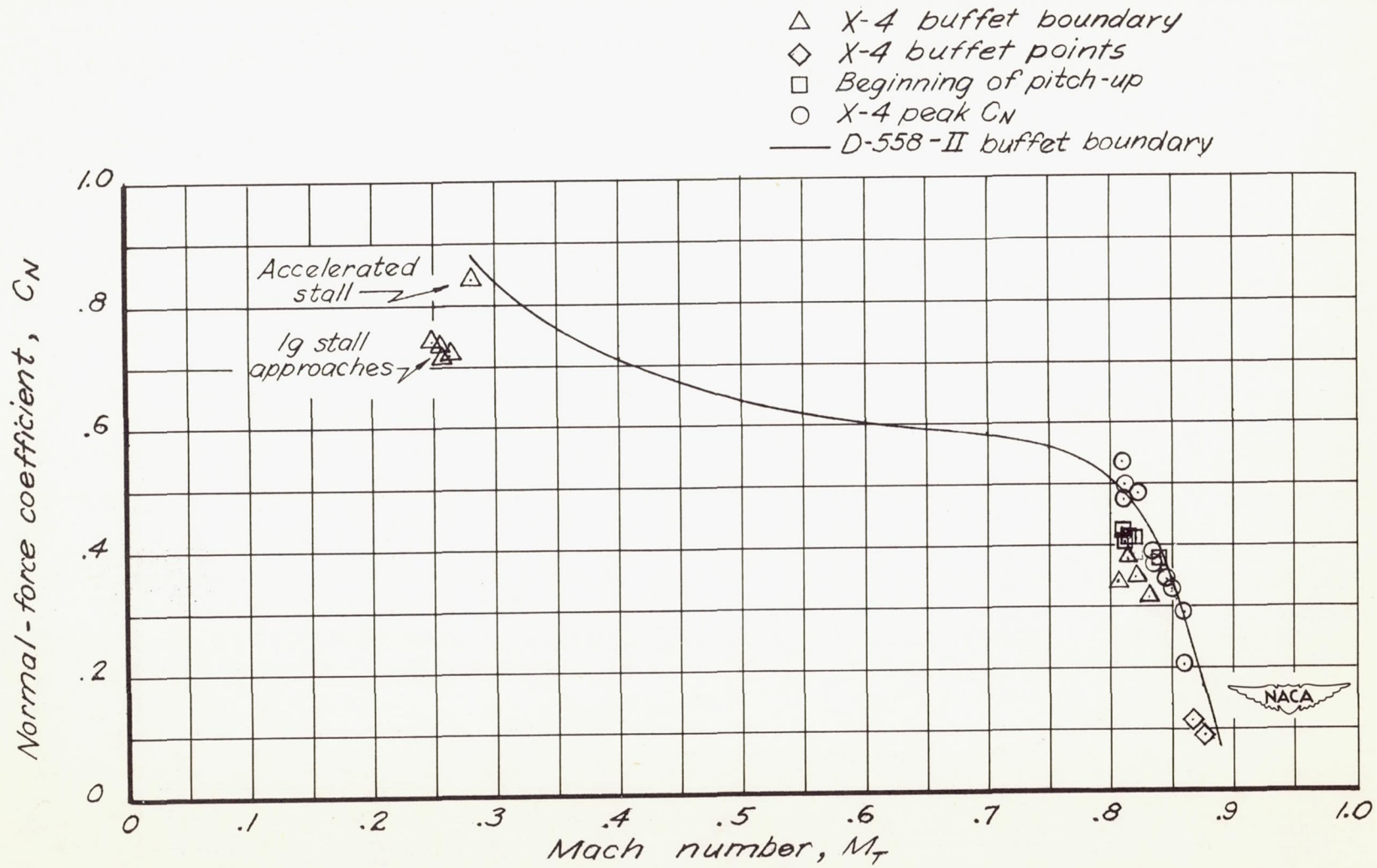


Figure 25.- Buffet boundary for X-4 airplane as determined from normal acceleration records.